PNAS RESEARCH ARTICLE | DEVELOPMENTAL BIOLOGY OPEN ACCESS

BRCA1 safeguards genome integrity by activating chromosome asynapsis checkpoint to eliminate recombination-defective oocytes

Long Bai[a,1], Peng Li[a,1], Yu Xiang[a,1], Xiaofei Jiao[a,b], Jiyuan Chen[a,b,2], Licun Song[a,b], Zhongyang Liang[a,b], Yidan Liu[c,3], Yimin Zhu[a,d,3], and Lin-Yu Lu[a,b,e,3]

Edited by Michael Lichten, NIH, Bethesda, MD; received February 2, 2024; accepted March 14, 2024

In the meiotic prophase, programmed DNA double-strand breaks are repaired by meiotic recombination. Recombination-defective meiocytes are eliminated to preserve genome integrity in gametes. BRCA1 is a critical protein in somatic homologous recombination, but studies have suggested that BRCA1 is dispensable for meiotic recombination. Here we show that BRCA1 is essential for meiotic recombination. Interestingly, BRCA1 also has a function in eliminating recombination-defective oocytes. *Brca1* knockout (KO) rescues the survival of *Dmc1* KO oocytes far more efficiently than removing CHK2, a vital component of the DNA damage checkpoint in oocytes. Mechanistically, BRCA1 activates chromosome asynapsis checkpoint by promoting ATR activity at unsynapsed chromosome axes in *Dmc1* KO oocytes. Moreover, *Brca1* KO also rescues the survival of asynaptic *Spo11* KO oocytes. Collectively, our study not only unveils an unappreciated role of chromosome asynapsis in eliminating recombination-defective oocytes but also reveals the dual functions of BRCA1 in safeguarding oocyte genome integrity.

homologous recombination | meiosis | chromosome asynapsis | oocyte

Genome integrity is paramount for gametes. Paradoxically, during the production of gametes, programmed DNA double-strand breaks (DSBs) are generated in the meiotic prophase and are repaired to facilitate crossover between homologous chromosomes, which are essential for proper chromosome alignment during metaphase I (1–3). Homologous recombination (HR) is exclusively used for DSB repair, and intricate checkpoints have evolved in the meiotic prophase to eliminate cells that are defective in meiotic recombination. The meiotic prophase checkpoints function in spermatocytes and oocytes, but more studies have been performed on oocytes (4–9).

After the completion of meiotic recombination at birth, oocytes are arrested at dictyate stages of the meiotic prophase. A layer of granulosa cells surrounds them to form primordial follicles, the only sources of oocytes during the entire female reproductive lifespan. To ensure oocyte quality, recombination-defective oocytes, such as *Dmc1*$^{-/-}$ oocytes, are eliminated before establishing a primordial follicle pool (4). Blocking programmed DSB formation by ablating SPO11 in *Dmc1*$^{-/-}$ oocytes reduces the efficiency of oocyte elimination (4), suggesting that unrepaired DSBs directly activate DNA damage checkpoint to eliminate recombination-defective oocytes. CHK2 is a critical component of the DNA damage checkpoint in oocytes, which triggers oocyte apoptosis through p53, p63, and BCL-2 family proteins (5, 8, 10, 11). *Chk2*$^{-/-}$ partially rescues the survival of recombination-defective oocytes, including *Dmc1*$^{-/-}$ oocytes (5).

Besides programmed DSBs, ionizing radiation (IR)-induced DSBs also activate DNA damage checkpoint to eliminate oocytes (5–8). *Chk2*$^{-/-}$ mice have unaltered oocyte number and unperturbed fertility after the same dose of IR that efficiently eliminates most oocytes in WT mice (5), suggesting that the DNA damage checkpoint is predominantly activated by CHK2-dependent pathways in oocytes. On the contrary, *Chk2*$^{-/-}$ inefficiently rescues the survival of *Dmc1*$^{-/-}$ oocytes, as *Dmc1*$^{-/-}$ *Chk2*$^{-/-}$ ovaries contain little primordial follicles and become atrophied within 2 mo (5). In the absence of CHK2, CHK1 might also contribute to the elimination of a subset of recombination-defective oocytes (10, 12), but it has not been formally examined whether *Chk1*$^{-/-}$ can rescue the survival of *Dmc1*$^{-/-}$ oocytes. Alternatively, DNA damage checkpoint might not be the major checkpoint for eliminating recombination-defective oocytes.

Besides unrepaired DSBs, recombination-defective oocytes manifest pervasive chromosome synapsis defects (asynapsis). Limited chromosome asynapsis (<3 pairs of asynaptic chromosomes) triggers oocyte elimination by suppressing the expression of essential genes through meiotic silencing of unsynapsed chromatin (MSUC) (13, 14). It is still debatable if chromosome asynapsis activates a checkpoint to trigger the elimination of oocytes with

Significance

In the meiotic prophase, homologous recombination repairs programmed DNA double-strand breaks (DSBs) and promotes the synapsis and crossover between homologous chromosomes. In recombination-defective oocytes, DSBs and chromosome asynapsis persist. These oocytes are eliminated soon after birth to maintain genome integrity. BRCA1 is a DNA damage response protein thoroughly studied in somatic cells. In this study, we have identified two functions of BRCA1 during mammalian germline development: promoting meiotic recombination and eliminating recombination-defective oocytes. BRCA1 promotes chromosome asynapsis checkpoint, not canonical DNA damage checkpoint, to eliminate recombination-defective oocytes. Our study highlights the importance of chromosome asynapsis in triggering the elimination of recombination-defective oocytes.

The authors declare no competing interest.

This article is a PNAS Direct Submission.

[1]L.B., P.L., and Y.X. contributed equally to this work.

[2]Present address: Westlake Laboratory of Life Sciences and Biomedicine, Westlake University, Hangzhou, 310024, China.

[3]To whom correspondence may be addressed. Email: yidanliu@zju.edu.cn, zhuyim@zju.edu.cn, or lulinyu@zju.edu.cn.

This article contains supporting information online at https://www.pnas.org/lookup/suppl/doi:10.1073/pnas.2401386121/-/DCSupplemental.

Published May 2, 2024.

pervasive chromosome asynapsis, such as *Spo11*$^{-/-}$ oocytes (4, 6, 9). It is even more elusive if chromosome asynapsis has an active role in eliminating recombination-defective oocytes that contain both pervasive chromosome asynapsis and unrepaired DSBs, such as *Dmc1*$^{-/-}$ oocytes. Preferentially located at unsynapsed chromosome axes, HORMAD1 and HORMAD2 have a potential role in chromosome asynapsis checkpoint (6, 15–18). *Hormad2*$^{-/-}$ poorly rescues the survival of *Dmc1*$^{-/-}$ oocytes (6, 16), suggesting that HORMAD2 is not essential for eliminating recombination-defective oocytes. On the contrary, *Hormad1*$^{-/-}$ efficiently rescues the survival of *Dmc1*$^{-/-}$ oocytes (19), but HORMAD1 might not directly promote checkpoint activation. Instead, it is proposed that HORMAD1 and its regulator RNF212 suppress inter-sister chromatid recombination (IS recombination) such that DSBs persist and activate DNA damage checkpoint to trigger oocyte elimination (7). Nevertheless, given the presence of pervasive chromosome asynapsis, an investigation is required to clarify whether a chromosome asynapsis checkpoint is activated to eliminate recombination-defective oocytes.

Despite having many differences, meiotic recombination and somatic HR operate similarly and share many core proteins. Both processes are initiated by DSB end resection to generate single-stranded DNA, which is then bound by recombinases to promote strand invasion (20). As a critical protein in somatic HR, BRCA1 promotes DSB end resection and recombinase loading (21–24). However, studies have indicated that BRCA1 is not essential for meiotic recombination (25, 26). Most of these studies use a mouse model that deletes the exon 11 of the *Brca1* gene, which encodes around half of the amino acids in BRCA1. Although *Brca1*$\Delta^{11/}\Delta^{11}p53^{+/-}$ male mice are infertile and are defective in RAD51 loading, *Brca1*$\Delta^{11/}\Delta^{11}p53^{+/-}$ female mice are fertile with no defect in chromosome synapsis or crossover formation (25). In addition, both germ cell-specific *Brca1*$\Delta^{11/}\Delta^{11}$ mice and *Brca1*$\Delta^{11/}\Delta^{11}$ *53bp1*$^{-/-}$ mice manifest male-specific infertility, and no defects in recombinase loading are observed (26). Based on these observations, it is generally believed that BRCA1 is dispensable for meiotic recombination in both sexes (26, 27). On the contrary, BRCA1 localizes to unsynapsed chromosome axes in the meiotic prophase of both sexes and potentially mediates key functions there (13, 27). In particular, BRCA1 recruits ATR to unsynapsed chromosome axes in the XY body of male meiotic prophase and promotes meiotic sex chromosome inactivation (MSCI), a unique type of MSUC in males (27). Similarly, it is believed that BRCA1 activates MUSC and promotes the elimination of oocytes with limited chromosomes asynapsis (13).

It should be noted that the *Brca1*Δ^{11} allele does not disrupt the BRCA1 protein completely but encodes an internally truncated BRCA1 protein that retains most functional domains of BRCA1 (28, 29). Therefore, BRCA1Δ11 protein is a hypomorphic BRCA1 protein that might be sufficient for meiotic recombination. In this study, we have utilized *Brca1* KO (*Brca1*$^{-/-}$) mice to reexamine whether BRCA1 functions in meiotic recombination and have found that BRCA1 plays a pivotal role in meiotic recombination by promoting the recruitment of meiotic recombinases to DSBs. Interestingly, BRCA1 also has a function in eliminating recombination-defective oocytes by activating the chromosome asynapsis checkpoint. The dual functions of BRCA1 in the meiotic prophase make it indispensable for preserving genome integrity in oocytes.

Results

BRCA1 Is Essential for Both Male and Female Fertility. Although studies using *Brca1*$\Delta^{11/}\Delta^{11}$ mice conclude that BRCA1 is dispensable for meiotic recombination, the presence of hypomorphic BRCA1Δ11 protein in *Brca1*$\Delta^{11/}\Delta^{11}$ mice prompts us to revisit BRCA1's function in meiotic recombination using *Brca1*$^{-/-}$ mice. Early embryonic lethality prevents direct examination of meiosis in *Brca1*$^{-/-}$ mice. We have shown previously that *53bp1*$^{-/-}$ rescues the DNA end resection defects but not recombinase loading defects or HR efficiency in *Brca1*$^{-/-}$ cells and partially rescues the viability but not genomic instability of *Brca1*$^{-/-}$ mice (28). Since *53bp1*$^{-/-}$ mice were fully fertile, *Brca1*$^{-/-}$ *53bp1*$^{-/-}$ mice were utilized to investigate BRCA1's function in meiotic recombination. Similar to male *Brca1*$\Delta^{11/}\Delta^{11}$ *53bp1*$^{-/-}$ mice, male *Brca1*$^{-/-}$ *53bp1*$^{-/-}$ mice were infertile (*SI Appendix*, Fig. S1*A*). No spermatozoa were present in adult epididymis (*SI Appendix*, Fig. S1*B*). Their testis size and weight were reduced (*SI Appendix*, Fig. S1 *C* and *D*), and histology revealed meiotic arrest as no haploid spermatids were observed (*SI Appendix*, Fig. S1*E*). Interestingly, female *Brca1*$^{-/-}$ *53bp1*$^{-/-}$ mice were also infertile (Fig. 1*A*), but developing follicles and corpus luteum were readily observed in adult ovaries (Fig. 1*B*). Collectively, unlike male-specific infertility of *Brca1*$\Delta^{11/}\Delta^{11}$ *53bp1*$^{-/-}$ mice, both male and female *Brca1*$^{-/-}$ *53bp1*$^{-/-}$ mice were infertile.

***Brca1* KO Oocytes Fail to Support Early Embryonic Development Due to Chiasmata Loss and Chromosome Segregation Error.** To explore the reasons for infertility in female *Brca1*$^{-/-}$ *53bp1*$^{-/-}$ mice, we examined early embryonic development after mating them with wild-type (WT) male mice. *Brca1*$^{-/-}$ *53bp1*$^{-/-}$ oocytes were fertilized normally, and the zygotes developed to the two-cell stage without apparent delay (Fig. 1 *C-D*). However, only 30% of embryos developed into the eight-cell stage at embryonic day (E) 2.5, and only 10% developed into the morula/blastocyst stage at E3.5 (Fig. 1*D*). To examine the intrinsic defects in *Brca1*$^{-/-}$ *53bp1*$^{-/-}$ oocytes that underlie the abnormal embryonic development, we analyzed oocytes at metaphase I and found that most exhibited misaligned chromosomes and aberrant spindle morphology (Fig. 1*E*). In agreement with this observation, severe aneuploidy was observed in most oocytes at metaphase II (Fig. 1*F*), suggesting that chromosomes were not segregated properly at metaphase I. Analysis of metaphase I chromosomes revealed that most *Brca1*$^{-/-}$ *53bp1*$^{-/-}$ oocytes contained primarily univalent (Fig. 1*G*). In contrast, most *53bp1*$^{-/-}$ oocytes had 20 bivalents connected by chiasmata, structures that link paired homologous chromosomes and maintain their proper alignment at metaphase I (Fig. 1*G*). Therefore, chiasmata loss is likely responsible for chromosome segregation error in *Brca1*$^{-/-}$ *53bp1*$^{-/-}$ oocytes.

BRCA1 Promotes Meiotic Recombinase Loading during Meiotic Recombination. Chiasmata are sites of crossover between homologous chromosomes, which are marked by MLH1 in the meiotic prophase. Consistent with chiasmata loss, crossover formation was largely abolished as MLH1 foci were dramatically reduced in the meiotic prophase of *Brca1*$^{-/-}$ *53bp1*$^{-/-}$ oocytes (Fig. 2*A*). Chromosome asynapsis was also observed, and only pachytene-like and diplotene-like stages could be observed (Fig. 2*B*). Chromosome asynapsis was further confirmed by the absence of SYCP1, the central element of the synaptonemal complex, and the presence of HORMAD1, chromosome synapsis surveillance protein, on many chromosomes (Fig. 2 *C* and *D*).

The above observations prompted us to investigate meiotic DSB repair, which is required for chromosome synapsis and crossover formation. In *Brca1*$^{-/-}$ *53bp1*$^{-/-}$ oocytes, DSB generation was normal since γH2AX signals in leptotene stages were indistinguishable from those in *53bp1*$^{-/-}$ oocytes (Fig. 2*B*). In *53bp1*$^{-/-}$ oocytes, the completion of DSB repair in pachytene stages was accompanied by diminishing γH2AX signals (Fig. 2*B*). However, in pachytene-like and diplotene-like stages of *Brca1*$^{-/-}$ *53bp1*$^{-/-}$ oocytes, γH2AX

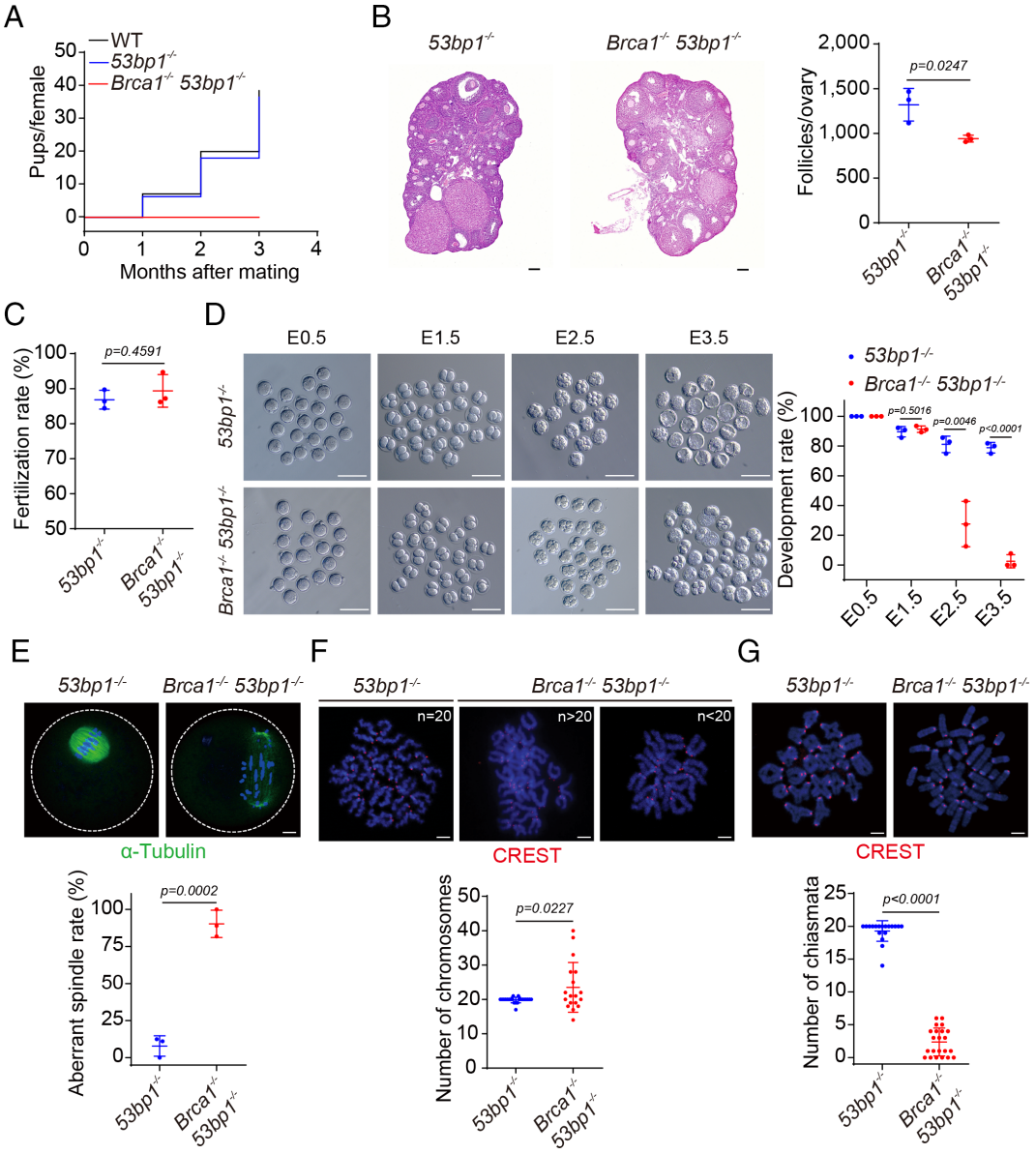

Fig. 1. BRCA1 is essential for female fertility and the euploidy of oocytes. (*A*) Cumulative number of pups per female obtained by mating WT, *53bp1*$^{-/-}$, and *Brca1*$^{-/-}$ *53bp1*$^{-/-}$ adult female mice with WT males for 3 consecutive months. Three females of each genotype are used for mating. (*B*) H&E staining of paraffin sections from *53bp1*$^{-/-}$ and *Brca1*$^{-/-}$ *53bp1*$^{-/-}$ ovaries at PD60. (Scale bars, 100 μm.) Quantification of follicles is shown on the right. (*C*) The fertilization rate of oocytes collected from *53bp1*$^{-/-}$and *Brca1*$^{-/-}$ *53bp1*$^{-/-}$ females. (*D*) Representative images of embryos collected from *53bp1*$^{-/-}$ and *Brca1*$^{-/-}$ *53bp1*$^{-/-}$ females at indicated time points after mating with WT males. E0.5/1.5/2.5/3.5 represent 0.5/1.5/2.5/3.5 d post coitum. (Scale bars, 100 μm.) The development rate of embryos is shown on the right. (*E*) Representative images of spindle morphology and chromosome alignment of in vitro matured oocytes from *53bp1*$^{-/-}$ and *Brca1*$^{-/-}$ *53bp1*$^{-/-}$ females. (Scale bars, 10 μm.) The aberrant spindle rate of in vitro matured oocytes is shown below. (*F*) Representative images of CREST staining in chromosome spreads of metaphase II oocytes from *53bp1*$^{-/-}$ and *Brca1*$^{-/-}$ *53bp1*$^{-/-}$ females. (Scale bars, 10 μm.) Quantification of chromosomes in chromosome spreads of metaphase II oocytes are shown below. (*G*) Representative images of CREST staining in chromosome spreads of metaphase I oocytes from *53bp1*$^{-/-}$ and *Brca1*$^{-/-}$ *53bp1*$^{-/-}$ females. (Scale bars, 10 μm.) Quantification of chiasmata in chromosome spreads of metaphase I oocytes are shown below.

signals were still abundant on many chromosomes (Fig. 2*B*), suggesting that DSBs were not fully repaired yet. DSBs are repaired by HR in the meiotic prophase. Consistent with BRCA1's active role in HR in somatic cells, *Brca1*$^{-/-}$ *53bp1*$^{-/-}$ oocytes had reduced foci number of meiotic recombinases RAD51 and DMC1 (Fig. 2 *E* and *F*), suggesting that these oocytes are deficient in meiotic recombination. On the contrary, *Brca1*$^{-/-}$ *53bp1*$^{-/-}$ oocytes had a similar number of RPA2 foci as those in *53bp1*$^{-/-}$ oocytes (Fig. 2*G*), suggesting that DNA end resection was intact in these oocytes.

Meiotic recombination is required for both male and female mice. In agreement with the observations in oocytes, defects in chromosome synapsis, DSB repair, and meiotic recombinase loading, but not DNA end resection were observed in *Brca1*$^{-/-}$ *53bp1*$^{-/-}$ spermatocytes (*SI Appendix*, Fig. S2). Therefore, unlike the conclusions drawn by previous studies, BRCA1 plays a pivotal role in meiotic recombination.

Loss of BRCA1 and 53BP1 Disrupts the Elimination of Recombination-Defective Oocytes. Recombination-defective oocytes are eliminated before the primordial follicle pool is established to maintain genomic integrity (4). Interestingly, although female *Brca1*$^{-/-}$ *53bp1*$^{-/-}$ mice had severe meiotic recombination defects, histology of adult ovaries did not reveal any apparent abnormalities (Fig. 1*B*). Further examination of ovaries at postnatal day (PD) 21 showed that the numbers of follicles in *Brca1*$^{-/-}$ *53bp1*$^{-/-}$ mice were slightly fewer than those in WT mice (Fig. 3*A*). This is in sharp contrast to *Dmc1*$^{-/-}$ female mice, which also had severe meiotic recombination defects, and no follicles could be observed in the atrophied ovaries at PD21 (Fig. 3*A*). At PD4, 1 d before the establishment of the primordial follicle pool, almost no oocytes could be identified in *Dmc1*$^{-/-}$ ovaries, but many oocytes were present in *Brca1*$^{-/-}$ *53bp1*$^{-/-}$ ovaries (Fig. 3*B*). These observations suggest that the meiotic recombination defects fail to trigger the elimination of *Brca1*$^{-/-}$ *53bp1*$^{-/-}$ oocytes.

Previous studies have found that recombination-defective oocytes are eliminated through CHK2-dependent DNA damage checkpoint, and *Chk2*$^{-/-}$ partially rescues the survival of *Dmc1*$^{-/-}$ oocytes (5). To examine whether BRCA1 and/or 53BP1 participate in these pathways, we generated *Dmc1*$^{-/-}$ *Brca1*$^{-/-}$ *53bp1*$^{-/-}$ mice. *Dmc1*$^{-/-}$ *Chk2*$^{-/-}$ mice were also generated for comparison. Similar to *Chk2*$^{-/-}$, *Brca1*$^{-/-}$ *53bp1*$^{-/-}$ partially rescued the survival of *Dmc1*$^{-/-}$ oocytes (Fig. 3*C*). Interestingly, *Dmc1*$^{-/-}$ *Brca1*$^{-/-}$ *53bp1*$^{-/-}$ ovaries

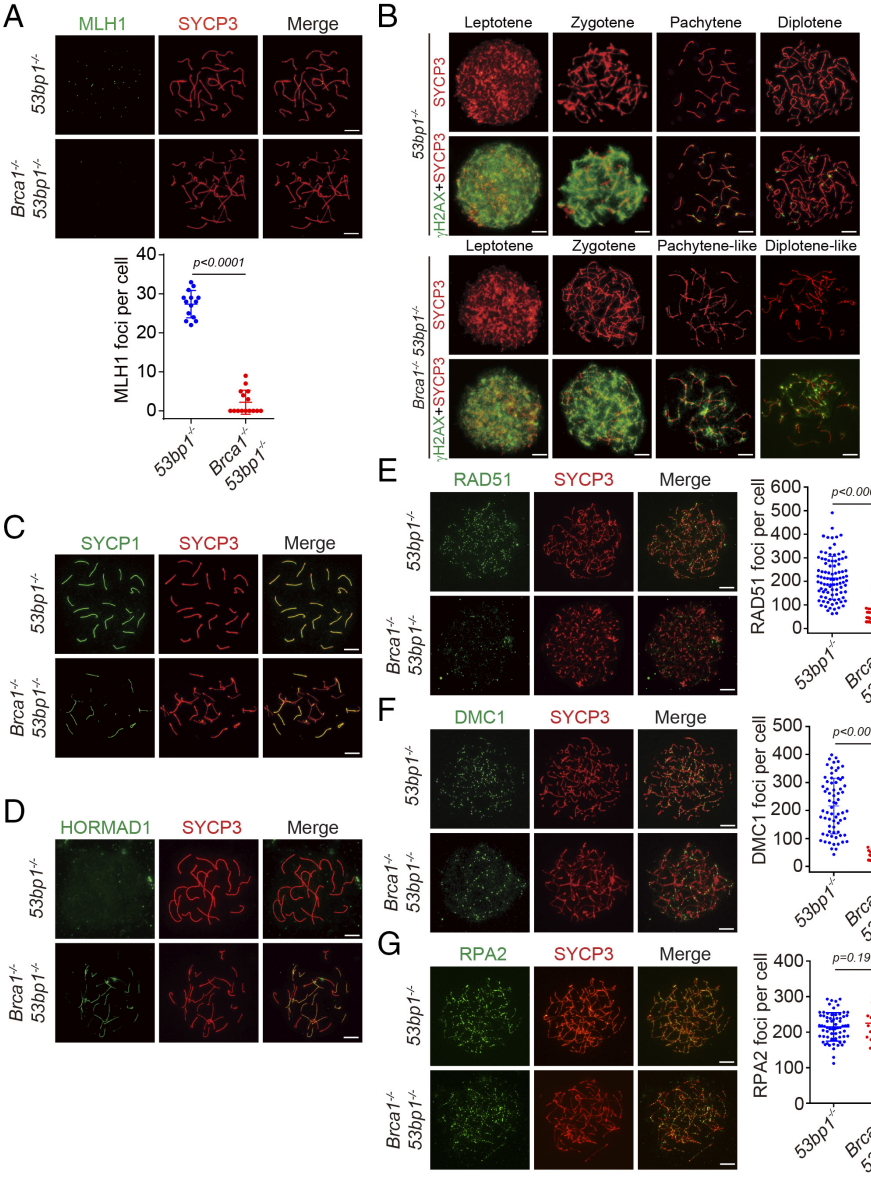

Fig. 2. BRCA1 promotes meiotic recombinase loading during meiotic recombination in oocytes. (*A*) Representative images of MLH1 and SYCP3 staining in chromosome spread of oocytes at E16.5 from *53bp1*$^{-/-}$ and *Brca1*$^{-/-}$ *53bp1*$^{-/-}$ females. (Scale bars, 10 μm.) Quantification of MLH1 foci in chromosome spread of oocytes are shown below. (*B*) Representative images of γH2AX and SYCP3 staining in chromosome spread of oocytes at E18.5 from *53bp1*$^{-/-}$ and *Brca1*$^{-/-}$ *53bp1*$^{-/-}$ females. (Scale bars, 10 μm.) (*C*) Representative images of SYCP1 and SYCP3 staining in chromosome spread of oocytes at E18.5 from *53bp1*$^{-/-}$and *Brca1*$^{-/-}$ *53bp1*$^{-/-}$ females. (Scale bars, 10 μm.) (*D*) Representative images of HORMAD1 and SYCP3 staining in chromosome spread of oocytes at E16.5 from *53bp1*$^{-/-}$ and *Brca1*$^{-/-}$ *53bp1*$^{-/-}$ females. (Scale bars, 10 μm.) (*E*) Representative images of RAD51 and SYCP3 staining in chromosome spread of oocytes at E14.5 from *53bp1*$^{-/-}$ and *Brca1*$^{-/-}$ *53bp1*$^{-/-}$ females. (Scale bars, 10 μm.) Quantification of RAD51 foci are shown on the right. (*F*) Representative images of DMC1 and SYCP3 staining in chromosome spread of oocytes at E14.5 from *53bp1*$^{-/-}$ and *Brca1*$^{-/-}$ *53bp1*$^{-/-}$ females. (Scale bars, 10 μm.) Quantification of DMC1 foci are shown on the right. (*G*) Representative images of RPA2 and SYCP3 staining in chromosome spread of oocytes at E14.5 from *53bp1*$^{-/-}$ and *Brca1*$^{-/-}$ *53bp1*$^{-/-}$ females. (Scale bars, 10 μm.) Quantification of RPA2 foci is shown on the right.

contained much more follicles than *Dmc1*$^{-/-}$ *Chk2*$^{-/-}$ ovaries at PD21 (Fig. 3*C*). Similar to previous studies, there were few primordial follicles in *Dmc1*$^{-/-}$ *Chk2*$^{-/-}$ ovaries at PD21 (Fig. 3*C*), and almost no follicles were present at PD60 (Fig. 3*D*). However, *Dmc1*$^{-/-}$ *Brca1*$^{-/-}$ *53bp1*$^{-/-}$ ovaries contained many primordial follicles at PD21 (Fig. 3*C*), and plenty of follicles were still present at PD60 (Fig. 3*D*). These observations suggest that *Brca1*$^{-/-}$ *53bp1*$^{-/-}$ rescues survival of *Dmc1*$^{-/-}$ oocytes with even greater efficiency than *Chk2*$^{-/-}$. Indeed, much more oocytes were present in *Dmc1*$^{-/-}$ *Brca1*$^{-/-}$ *53bp1*$^{-/-}$ ovaries than in *Dmc1*$^{-/-}$ *Chk2*$^{-/-}$ ovaries at PD4 (Fig. 3*E*). Collectively, loss of BRCA1 and 53BP1 significantly disrupts the oocyte elimination pathway and permits the survival of recombination-defective oocytes. It should be noted that the survived oocytes cannot support embryonic development when fertilized due to crossover defects.

BRCA1 Is Required for the Elimination of Recombination-Defective Oocytes. To identify the protein whose loss was responsible for the oocyte elimination defect in *Brca1*$^{-/-}$ *53bp1*$^{-/-}$ mice, we examined the fate of *Dmc1*$^{-/-}$ oocytes when BRCA1 and 53BP1 were lost individually. Similar to *Dmc1*$^{-/-}$, *Dmc1*$^{-/-}$ *53bp1*$^{-/-}$ mice had atrophied ovaries that contained almost no follicles at PD21 (Fig. 4*A*), suggesting that 53BP1 has no active role in the elimination of recombination-defective oocytes.

Since *Brca1*$^{-/-}$ mice are embryonic lethal, germ cell-specific *Brca1*$^{-/-}$ needs to be generated to examine the role of BRCA1 in eliminating recombination-defective oocytes. Given that the ovaries of newborn *Dmc1*$^{-/-}$ mice contain fewer oocytes than those of WT mice (4), the elimination of recombination-defective oocytes likely starts at the embryonic stages. Therefore, *Brca1* should be deleted in embryonic oocytes as early as possible to achieve the best effects. We selected *Stra8-GFPCre* mice in which a GFP-tagged Cre recombinase is expressed under the control of endogenous *Stra8* gene promoter (30). In female mice, the GFP-Cre fusion protein is expressed at the same time when STRA8 is expressed before meiotic entry at E13.5 (*SI Appendix*, Fig. S3 *A*–*C*). Unlike *Brca1*$^{-/-}$ *53bp1*$^{-/-}$ mice, female *Brca1*$^{f/-}$ *Stra8-GFPCre* mice were fertile (*SI Appendix*, Fig. S3 *D* and *E*), and no defects in meiotic progression, DNA end resection, or meiotic recombinase loading were observed (*SI Appendix*, Fig. S4). Since BRCA1 was still detectable in oocytes at early leptotene (*SI Appendix*, Fig. S5), it is possible that the BRCA1 protein is not fully degraded so that sufficient protein is present when its function is required at leptotene stages (*Discussion*).

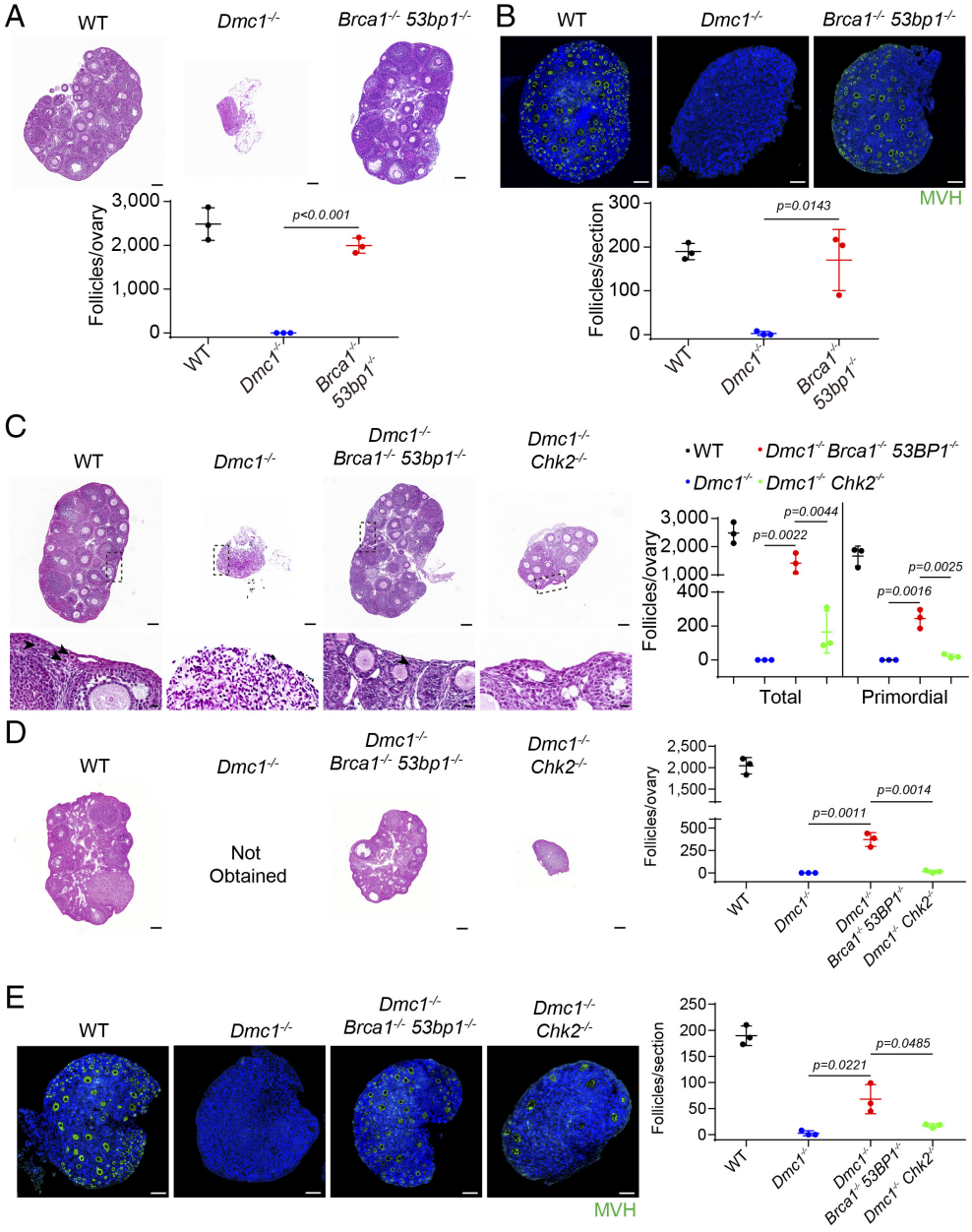

Fig. 3. Loss of BRCA1 and 53BP1 disrupts the elimination of recombination-defective oocytes. (*A*) H&E staining of paraffin sections from *53bp1*$^{-/-}$ and *Brca1*$^{-/-}$ *53bp1*$^{-/-}$ ovaries at PD21. (Scale bars, 100 μm.) Quantification of follicles are shown below. (*B*) Representative images of MVH staining in paraffin sections of ovaries from WT, *Dmc1*$^{-/-}$, and *Brca1*$^{-/-}$ *53bp1*$^{-/-}$ females at PD4. (Scale bars, 10 μm.) Quantification of follicles per section is shown below. (*C*) H&E staining of paraffin sections from WT, *Dmc1*$^{-/-}$, *Dmc1*$^{-/-}$ *Brca1*$^{-/-}$ *53bp1*$^{-/-}$, and *Dmc1*$^{-/-}$ *Chk2*$^{-/-}$ovaries at PD21. Black dotted boxes in *Upper* panels were magnified in *Lower* panels. Black arrowheads in *Lower* panels indicate primordial follicles. (Scale bars in *Upper* panels, 100 μm; Scale bars in *Lower* panels, 5 μm.) Quantification of total follicles and primordial follicles are shown on the right. (*D*) H&E staining of paraffin sections from WT, *Dmc1*$^{-/-}$ *Brca1*$^{-/-}$ *53bp1*$^{-/-}$, and *Dmc1*$^{-/-}$ *Chk2*$^{-/-}$ ovariesat PD60. (Scale bars, 100 μm.) Quantification of follicles are shown on the right. (*E*) Representative images of MVH staining in paraffin sections of ovaries from WT, *Dmc1*$^{-/-}$, *Dmc1*$^{-/-}$ *Brca1*$^{-/-}$ *53bp1*$^{-/-}$, and *Dmc1*$^{-/-}$ *Chk2*$^{-/-}$ females at PD4. (Scale bars, 10 μm.) Quantification of follicles per section is shown on the right.

Nevertheless, BRCA1 was undetectable in oocytes at late leptotene stages and beyond (*SI Appendix*, Fig. S5), allowing us to examine whether removing BRCA1 rescues the survival of *Dmc1*$^{-/-}$ oocytes.

Similar to *Brca1*$^{-/-}$ *53bp1*$^{-/-}$, *Brca1*$^{f/-}$ *Stra8-GFPCre* partially rescued the survival of *Dmc1*$^{-/-}$ oocytes with greater efficiency than *Chk2*$^{-/-}$ (Fig. 4*A*). The number of total follicles and primordial follicles in *Dmc1*$^{-/-}$ *Brca1*$^{f/-}$ *Stra8-GFPCre* ovaries at PD21 were comparable to those in *Dmc1*$^{-/-}$ *Brca1*$^{-/-}$ *53bp1*$^{-/-}$ ovaries (Figs. 3*C* and 4*A*). Consistently, *Dmc1*$^{-/-}$ *Brca1*$^{f/-}$ *Stra8-GFPCre* ovaries still contained plenty of growing follicles at PD60 and many oocytes at PD4 (Fig. 4 *B* and *C*). Therefore, germ cell-specific *Brca1*$^{-/-}$ was as efficient as *Brca1*$^{-/-}$ *53bp1*$^{-/-}$ in rescuing the survival of *Dmc1*$^{-/-}$ oocytes. These observations suggest that BRCA1 is the key protein to eliminate recombination-defective oocytes.

BRCA1 Does Not Activate DNA Damage Checkpoint but Promotes ATR Activity on Unsynapsed Chromosome Axes of Recombination-Defective Oocytes. To explore how BRCA1 promotes the elimination of *Dmc1*$^{-/-}$ oocytes, we first examined whether it functions similarly as CHK2 does to activate DNA damage checkpoint in *Dmc1*$^{-/-}$ oocytes. Using IR-induced DSBs in WT oocytes to mimic programmed DSBs in *Dmc1*$^{-/-}$ oocytes, it has been shown that IR triggers the elimination of most oocytes in WT ovaries (5–8). Consistent with previous studies and our observation that *Chk2*$^{-/-}$ partially rescues the survival of *Dmc1*$^{-/-}$ oocytes, most oocytes remained intact in *Chk2*$^{-/-}$ ovaries after IR (Fig. 5*A*). On the contrary, most oocytes were eradicated by IR in *Brca1*$^{f/-}$ *Stra8-GFPCre* ovaries (Fig. 5*A*), suggesting that BRCA1 has little function in DNA damage checkpoint in oocytes. To consolidate this finding, we tested whether *Brca1*$^{-/-}$ compromises any signaling pathways in DNA damage checkpoint in oocytes. DNA damage checkpoint is predominantly activated by CHK2-dependent pathways in oocytes, including phosphorylation and activation of oocyte-specific protein p63 (5). Consistent with previous studies, IR induced p63 phosphorylation and mobility shift in WT ovaries but not in *Chk2*$^{-/-}$ ovaries (Fig. 5*B*). Like in WT ovaries, IR robustly induced p63 phosphorylation in *Brca1*$^{f/-}$ *Stra8-GFPCre* ovaries (Fig. 5*B*), suggesting BRCA1 does not regulate IR-induced CHK2-dependent pathways in oocytes.

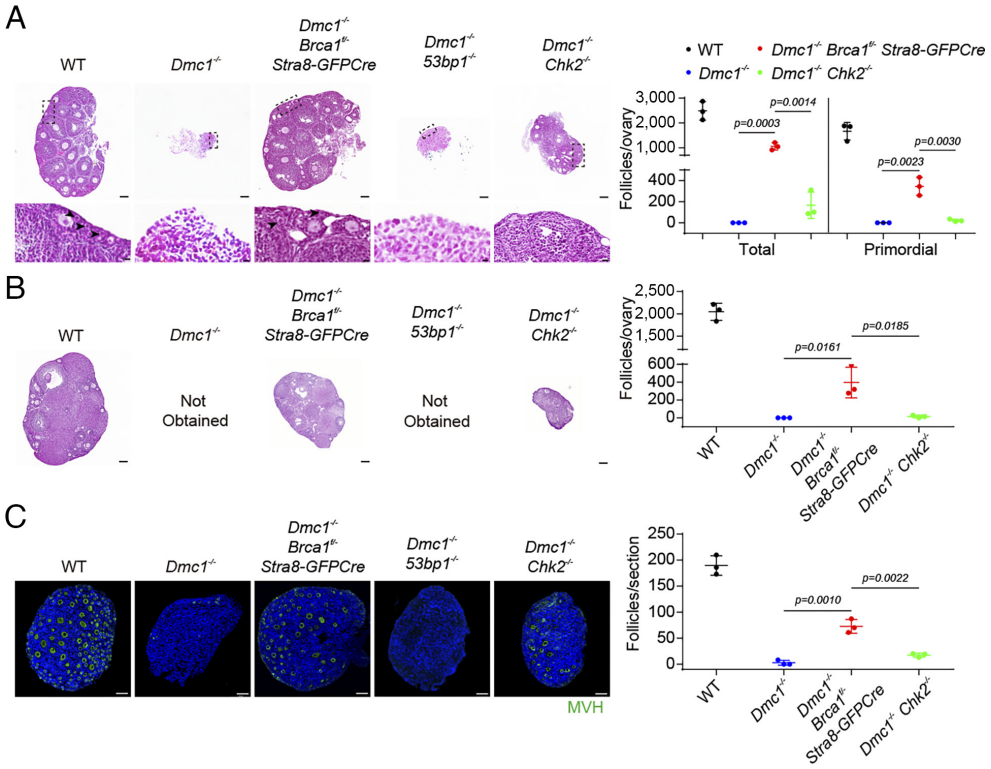

Fig. 4. BRCA1 is required for the elimination of recombination-defective oocytes. (*A*) H&E staining of paraffin sections from WT, *Dmc1*$^{-/-}$, *Dmc1*$^{-/-}$ *Brca1*$^{f/-}$ *Stra8-GFPCre*, *Dmc1*$^{-/-}$ *53bp1*$^{-/-}$, and *Dmc1*$^{-/-}$ *Chk2*$^{-/-}$ ovaries at PD21. Black dotted boxes in *Upper* panels were magnified in *Lower* panels. Black arrowheads indicate primordial follicles. (Scale bars in *Upper* panels, 100 μm; Scale bars in *Lower* panels, 5 μm.) Quantification of total follicles and primordial follicles are shown on the right. (*B*) H&E staining of paraffin sections from WT, *Dmc1*$^{-/-}$ *Brca1*$^{f/-}$ *Stra8-GFPCre*, and *Dmc1*$^{-/-}$ *Chk2*$^{-/-}$ ovaries at PD60. (Scale bars, 100 μm.) Quantification of follicles are shown on the right. (*C*) Representative images of MVH staining in paraffin sections of ovaries from WT, *Dmc1*$^{-/-}$, *Dmc1*$^{-/-}$ *Brca1*$^{f/-}$ *Stra8-GFPCre*, *Dmc1*$^{-/-}$ *53bp1*$^{-/-}$, and *Dmc1*$^{-/-}$ *Chk2*$^{-/-}$ females at PD4. (Scale bars, 10 μm.) Quantification of follicles per section is shown on the right.

Besides CHK2, CHK1 is another DNA damage checkpoint kinase that potentially participates in the elimination of recombination-defective oocytes (10, 12). Unlike p63, CHK1 is not specifically expressed in oocytes, but IR robustly induced the signal of p-CHK1(S317), a phosphorylation event associated with CHK1 activation, in oocytes but not in somatic cells in WT ovaries (Fig. 5*C*). Together with the observation that IR specifically eradicates oocytes but not somatic cells in WT ovaries, these findings indicate that the DNA damage checkpoint is much more sensitive in oocytes than in somatic cells. In *Brca1*$^{f/-}$ *Stra8-GFPCre* ovaries, the p-CHK1(S317) signal was also robustly induced by IR (Fig. 5*C*), suggesting that BRCA1 does not regulate IR-induced CHK1 activation in oocytes. These observations collectively indicate that the signaling pathways in the DNA damage checkpoint are intact in *Brca1*$^{f/-}$ *Stra8-GFPCre* oocytes. Therefore, unlike CHK2, BRCA1 does not have an active role in DNA damage checkpoint in oocytes.

In recombination-defective oocytes, unrepaired DSBs are often accompanied by chromosome asynapsis. In spermatocytes, BRCA1 localizes to unsynapsed chromosome axes and regulates the recruitment of ATR, particularly in the XY body (27, 31). Since ATR activity could also be observed on unsynapsed chromosome axes in oocytes (31, 32), we examined whether ATR activity is regulated by BRCA1 in oocytes, especially in recombination-defective oocytes. We analyzed the localization of p-HORMAD2(S271), an established ATR substrate on unsynapsed chromosome axes (9, 31). p-HORMAD2(S271) could be readily detected in the meiotic prophase of WT oocytes, which were located at unsynapsed chromosome axes at zygotene stages and disappeared when chromosomes fully synapsed at pachytene stages (Fig. 5*D*). In newborn (PD0) *Dmc1*$^{-/-}$ oocytes, p-HORMAD2(S271) were also present on unsynapsed chromosome axes, and the signals were dramatically decreased in PD0 *Dmc1*$^{-/-}$ *Brca1*$^{f/-}$ *Stra8-GFPCre* oocytes but not in PD0 *Dmc1*$^{-/-}$ *Chk2*$^{-/-}$ oocytes (Fig. 5*E*). Therefore, the ATR activity on unsynapsed chromosome axes of PD0 *Dmc1*$^{-/-}$ oocytes requires BRCA1 but not CHK2, suggesting that BRCA1 promotes the elimination of recombination-defective oocytes by regulating ATR activity on unsynapsed chromosome axes independently of CHK2.

We continued to examine whether BRCA1 regulates ATR's localization in recombination-defective oocytes. Unexpectedly, we failed to reliably detect ATR signals on unsynapsed chromosome axes of PD0 WT or *Dmc1*$^{-/-}$ oocytes, despite the fact that robust ATR signals could be observed in the XY body in spermatocytes (*SI Appendix*, Fig. S6 *A* and *B*). As an enzyme, ATR might transiently localize to unsynapsed chromosome axes to phosphorylate its substrates. Therefore, we examined ATR's localization in oocytes at embryonic stages. Indeed, ATR could be observed on unsynapsed chromosome axes of E16.5 *Dmc1*$^{-/-}$ oocytes (Fig. 5*F*), and ATR signal was dramatically decreased in E16.5 *Dmc1*$^{-/-}$ *Brca1*$^{f/-}$ *Stra8-GFPCre* oocytes (Fig. 5*F*). Consistent with this observation, the ATR signal on unsynapsed chromosome axes was dramatically decreased in E16.5 *Brca1*$^{-/-}$ *53bp1*$^{-/-}$ oocytes than that in E16.5 *53bp1*$^{-/-}$ oocytes (*SI Appendix*, Fig. S6*C*). Taken together, BRCA1 promotes ATR activity on unsynapsed chromosome axes of recombination-defective oocytes by regulating ATR's localization.

BRCA1 Functions Downstream of HORMAD1 on Unsynapsed Chromosome Axes but Does Not Suppress IS Recombination in Recombination-Defective Oocytes. It is noteworthy that ATR and its phosphorylated substrates were not restricted to sites of DSB but were present on the unsynapsed chromosome axes in oocytes (Fig. 5 *D*–*F*). Since BRCA1 promotes ATR activity on unsynapsed chromosome axes, BRCA1's function is unlikely restricted to DSB sites either. In spermatocytes, BRCA1 localizes at unsynapsed chromosome axes, particularly in the XY body (27). Careful examination of BRCA1's localization in oocytes revealed that BRCA1 was loaded onto unsynapsed chromosome axes very early in the leptotene stages (Fig. 6*A*). In zygotene stages, BRCA1 disappeared from SYCP1-positive regions where homologous chromosomes had synapsed. In pachytene stages, all chromosomes were fully synapsed, and BRCA1 could no longer be observed (Fig. 6*A*). The pattern of BRCA1's localization suggests

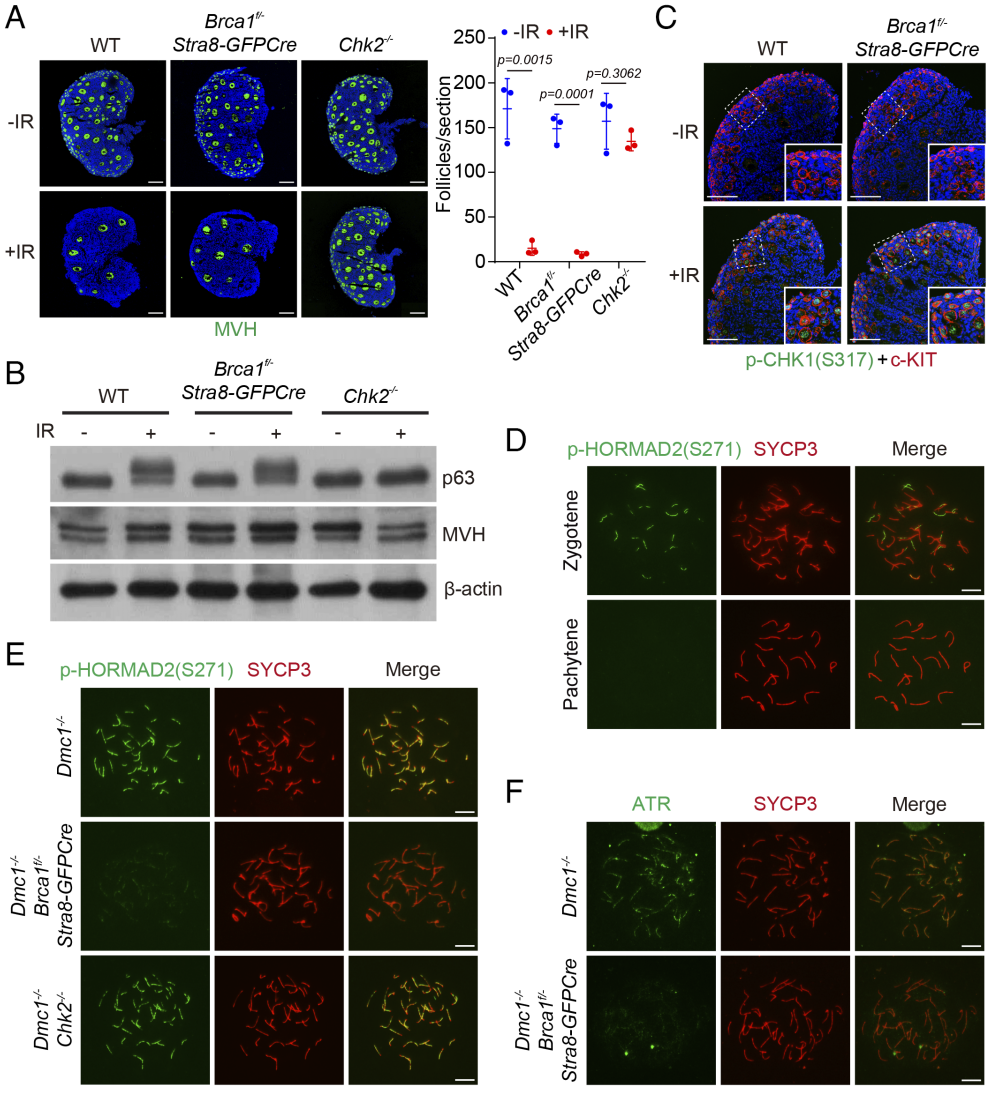

Fig. 5. BRCA1 does not activate DNA damage checkpoint but promotes ATR activity on unsynapsed chromosome axes of recombination-defective oocytes. (*A*) Representative images of MVH staining in ovarian sections at PD10 from WT, *Brca1*$^{f/-}$ *Stra8-GFPCre*, and *Chk2*$^{-/-}$ females after 0.45 Gy IR exposure at PD3. (Scale bars, 100 μm.) Quantification of follicles per section is shown on the right. (*B*) Western blotting analysis of p63 phosphorylation level of ovaries at PD3 from WT, *Brca1*$^{f/-}$ *Stra8-GFPCre*, and *Chk2*$^{-/-}$ females after 3 Gy IR exposure. MVH and β-actin serve as the internal loading controls. (*C*) Representative images of p-CHK1 (S317) and c-KIT staining in ovarian sections at PD3 from WT and *Brca1*$^{f/-}$ *Stra8-GFPCre* females after 3 Gy IR exposure. (Scale bars, 100 μm.) (*D*) Representative images of p-HORMAD2 (S271) and SYCP3 staining in chromosome spread of oocytes at PD0 from WT females. (Scale bars, 10 μm.) (*E*) Representative images of p-HORMAD2 (S271) and SYCP3 staining in chromosome spread of oocytes at PD0 from *Dmc1*$^{-/-}$, *Dmc1*$^{-/-}$ *Brca1*$^{f/-}$ *Stra8-GFPCre*, and *Dmc1*$^{-/-}$ *Chk2*$^{-/-}$females. (Scale bars, 10 μm.) (*F*) Representative images of ATR and SYCP3 staining in chromosome spread of oocytes at E16.5 from *Dmc1*$^{-/-}$ and *Dmc1*$^{-/-}$ *Brca1*$^{f/-}$ *Stra8-GFPCre* females. (Scale bars, 10 μm.)

that BRCA1 participates in the surveillance of chromosome synapsis, which mimics the behavior of HORMAD1. Indeed, BRCA1 colocalized with HORMAD1 in all stages of the meiotic prophase in oocytes (Fig. 6*B*).

Previous studies have shown that BRCA1 localizes at unsynapsed chromosome axes and initiates meiotic silencing of unsynapsed chromatin (MSUC) in oocytes with limited chromosome asynapsis (13). In PD0 *Dmc1*$^{-/-}$ oocytes that manifest pervasive chromosome asynapsis, BRCA1's signal was nonuniform but still covered most regions of unsynapsed chromosome axes of all chromosomes (Fig. 6*C*). Since BRCA1 is required to eliminate *Dmc1*$^{-/-}$ oocytes, BRCA1's localization and function are unlikely to be restricted by the number of unsynapsed chromosomes in oocytes. Similar to the observation in *Spo11*$^{-/-}$ spermatocytes (33), BRCA1 still localized at many unsynapsed chromosome axes in PD0 *Spo11*$^{-/-}$ oocytes that lacked programmed DSBs (Fig. 6*D*), further demonstrating that BRCA1 localizes at unsynapsed chromosome axes in a DSB-independent manner in oocytes.

Similar to *Brca1*$^{-/-}$, *Hormad1*$^{-/-}$ efficiently rescues the survival of *Dmc1*$^{-/-}$ oocytes (19). Previous studies have suggested that HORMAD1 regulates the localization of BRCA1 and ATR on unsynapsed chromosome axes (15), and we further examined the relationship between HORMAD1 and BRCA1 in oocytes. The localization of BRCA1 on unsynapsed chromosome axes was indeed largely abolished in *Hormad1*$^{-/-}$ oocytes (Fig. 6*E*). On the contrary, HORMAD1 remained at the unsynapsed chromosome axes in *Brca1*$^{f/-}$ *Stra8-GFPCre* oocytes (Fig. 6*F*). These observations suggest BRCA1 functions downstream of HORMAD1 to regulate ATR activity on unsynapsed chromosome axes in oocytes.

HORMAD1 suppresses IS recombination during the meiotic prophase. Removing HORMAD1 or its regulator RNF212 rescues the survival of recombination-defective oocytes by lifting the restriction on IS recombination so that unrepaired DSBs no longer accumulate (7). Since BRCA1 functions downstream of HORMAD1 on unsynapsed chromosome axes in oocytes, we examined whether loss of BRCA1 also rescued the survival of *Dmc1*$^{-/-}$ oocytes by permitting DSB repair through IS recombination. The numbers of RPA2 foci were present at similar levels in PD0 *Dmc1*$^{-/-}$ and *Dmc1*$^{-/-}$ *Brca1*$^{f/-}$ *Stra8-GFPCre* oocytes (Fig. 6*G*), suggesting that *Brca1*$^{-/-}$ rescues the survival of *Dmc1*$^{-/-}$ oocytes without promoting DSB repair. Therefore, BRCA1 has no active role in suppressing IS recombination. Instead, BRCA1-dependent ATR activity on unsynapsed chromosome axes triggers the elimination of recombination-defective oocytes independently of unrepaired DSBs.

BRCA1-Dependent ATR Activity on Unsynapsed Chromosome Axes Promotes the Elimination of *Spo11* KO Oocytes. In most recombination-defective oocytes such as *Dmc1*$^{-/-}$, unrepaired DSBs and chromosome asynapsis coexist. The observation

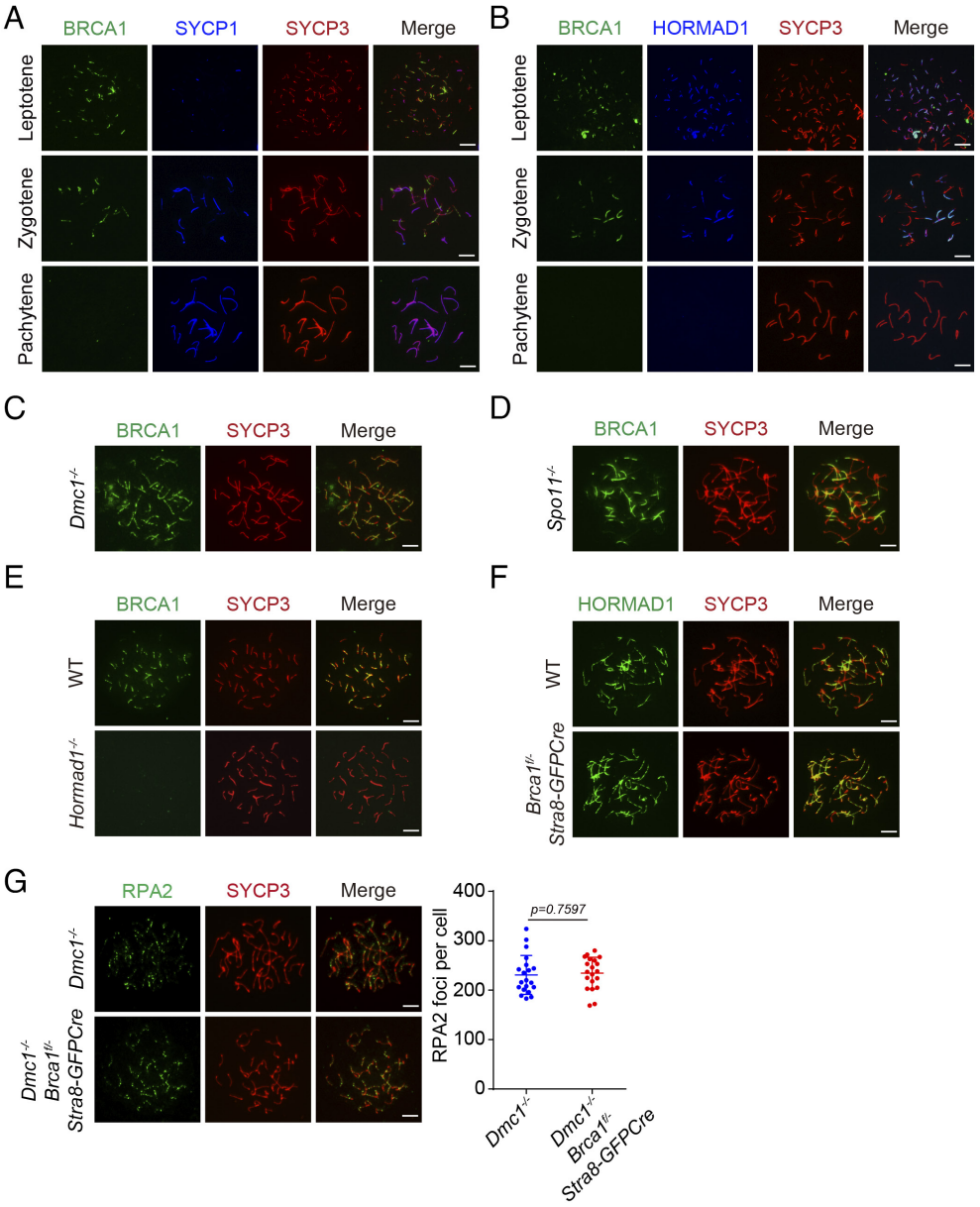

Fig. 6. BRCA1 functions downstream of HORMAD1 on unsynapsed chromosome axes but does not suppress IS recombination in recombination-defective oocytes. (*A*) Representative images of BRCA1, SYCP1, and SYCP3 staining in chromosome spread of oocytes at leptotene, zygotene, and pachytene from WT females. (Scale bars, 10 μm.) (*B*) Representative images of BRCA1, HORMAD1, and SYCP3 staining in chromosome spread of oocytes at leptotene, zygotene, and pachytene from WT females. (Scale bars, 10 μm.) (*C*) Representative images of BRCA1 and SYCP3 staining in chromosome spread of oocytes at PD0 from *Dmc1*$^{-/-}$females. (Scale bars, 10 μm.) (*D*) Representative images of BRCA1 and SYCP3 staining in chromosome spread of oocytes at PD0 from *Spo11*$^{-/-}$females. (Scale bars, 10 μm.) (*E*) Representative images of BRCA1 and SYCP3 staining in chromosome spread of oocytes at PD0 from WT and *Hormad1*$^{-/-}$ females. (Scale bars, 10 μm.) (*F*) Representative images of HORMAD1 and SYCP3 staining in chromosome spread of oocytes at E15.5 from WT and *Brca1*$^{-/-}$ *Stra8-GFPCre* females. (Scale bars, 10 μm.) (*G*) Representative images of RPA2 and SYCP3 staining in chromosome spread of oocytes at PD0 from *Dmc1*$^{-/-}$ and *Dmc1*$^{-/-}$ *Brca1*$^{f/-}$ *Stra8-GFPCre* females. (Scale bars, 10 μm.) Quantification of RPA2 foci are shown on the right.

that *Brca1*$^{-/-}$ rescues the survival of *Dmc1*$^{-/-}$ oocytes without promoting DSB repair highlights the significance of chromosome asynapsis in triggering oocyte elimination. To test this idea further, we examined whether the loss of BRCA1 rescued the survival of asynaptic *Spo11*$^{-/-}$ oocytes, in which no programmed DSBs are generated. *Spo11*$^{-/-}$ oocytes are also eliminated at birth, albeit less efficiently than *Dmc1*$^{-/-}$ oocytes. *Spo11*$^{-/-}$ ovaries were atrophied and devoid of follicles at PD60 (Fig. 7*A*). On the contrary, significant numbers of follicles, including primordial follicles, were present in *Spo11*$^{-/-}$ *Brca1*$^{f/-}$ *Stra8-GFPCre* ovaries at PD60 (Fig. 7*A*), demonstrating that *Brca1*$^{-/-}$ rescues the survival of *Spo11*$^{-/-}$ oocytes. Consistent with the presence of BRCA1 on unsynapsed chromosome axes in PD0 *Spo11*$^{-/-}$ oocytes, the ATR substrates p-HORMAD2(S271) was present on many unsynapsed chromosome axes of PD0 *Spo11*$^{-/-}$ oocytes, and it was diminished in PD0 *Spo11*$^{-/-}$ *Brca1*$^{f/-}$ *Stra8-GFPCre* oocytes (Fig. 7*B*). Therefore, BRCA1 also promotes ATR activity on unsynapsed chromosome axes of *Spo11*$^{-/-}$ oocytes. There are opposing views on whether DSBs of unknown origins trigger the elimination of *Spo11*$^{-/-}$ oocytes (6, 9, 34, 35). Since *Brca1*$^{-/-}$ does not promote DSB repair but rescues the survival of *Spo11*$^{-/-}$ oocytes, BRCA1-dependent ATR activity on unsynapsed chromosome axes likely triggers the elimination of *Spo11*$^{-/-}$ oocytes, no matter if DSBs are present in *Spo11*$^{-/-}$ oocytes or not. The observations in both *Dmc1*$^{-/-}$ and *Spo11*$^{-/-}$ oocytes collectively suggest that chromosome asynapsis is critical for eliminating recombination-defective oocytes.

Discussion

BRCA1 Is Indispensable for Meiotic Recombination. Studies using hypomorphic *Brca1Δ*$^{11/}$*Δ*^{11} mice have suggested that BRCA1 is largely dispensable for meiotic recombination (25, 26). Using bona fide *Brca1* null mice in this study, we demonstrate that BRCA1 is required for loading meiotic recombinases to DSBs during meiotic recombination. These opposite conclusions suggest that BRCA1Δ11 protein is generally sufficient for meiotic recombination, especially for loading meiotic recombinases to DSBs. Similarly, our previous study in somatic cells has shown that *Brca1*$^{-/-}$ *53bp1*$^{-/-}$ cells manifest severe HR deficiency (28), which is different from *Brca1Δ*$^{11/}$*Δ*^{11} *53bp1*$^{-/-}$ cells that are proficient in HR (36). Therefore, the function of the BRCA1Δ11

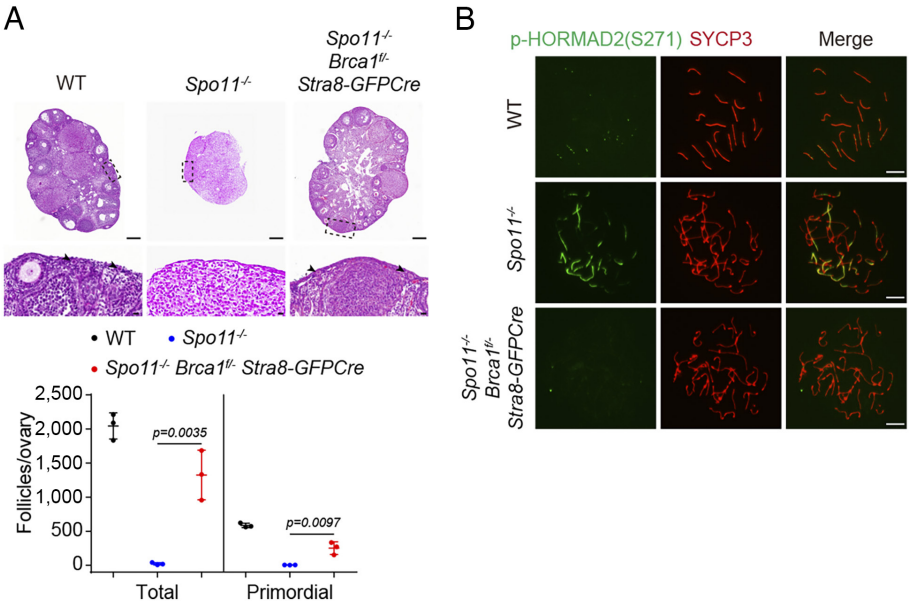

Fig. 7. BRCA1-dependent ATR activity on unsynapsed chromosome axes promotes the elimination of *Spo11* KO oocytes. (*A*) H&E staining of paraffin sections from WT, *Spo11*$^{-/-}$, and *Spo11*$^{-/-}$ *Brca1*$^{f/-}$ *Stra8-GFPCre* ovaries at PD60. Black dotted boxes in *Upper* panels were magnified in *Lower* panels. Black arrowheads indicate primordial follicles. (Scale bars in *Upper* panels, 100 μm; Scale bars in *Lower* panels, 5 μm.) Quantification of total follicles and primordial follicles are shown below. (*B*) Representative images of p-HORMAD2 (S271) and SYCP3 staining in chromosome spread of oocytes at PD0 from WT, *Spo11*$^{-/-}$, and *Spo11*$^{-/-}$ *Brca1*$^{f/-}$ *Stra8-GFPCre* females. (Scale bars, 10 μm.)

protein should be considered when interpreting the studies using hypomorphic *Brca1*Δ^{11}/Δ^{11} mice (37).

Besides recombinase loading, BRCA1 is required for DNA end resection in somatic cells. Interestingly, DNA end resection is normal in the meiotic prophase of *Brca1*Δ^{11}/Δ^{11} *p53*$^{+/-}$ male mice, despite the fact that *Brca1*Δ^{11}/Δ^{11} MEFs are defective in DNA end resection (38). Since *53bp1*$^{-/-}$ rescues the DNA end resection defects in *Brca1*$^{-/-}$ cells, the role of BRCA1 in meiotic DNA end resection cannot be studied using *Brca1*$^{-/-}$ *53bp1*$^{-/-}$ mice. Unlike female *Brca1*$^{-/-}$ *53bp1*$^{-/-}$ mice, female *Brca1*$^{f/-}$ *Stra8-GFPCre* mice are fertile and have no defects in meiotic progression, DNA end resection, or meiotic recombinase loading. Since BRCA1 was still detectable in oocytes at early leptotene (*SI Appendix*, Fig. S5), it is possible that the BRCA1 protein is not fully degraded so that sufficient protein is present when its function is required at leptotene stages. Therefore, female *Brca1*$^{f/-}$ *Stra8-GFPCre* mice are not suitable for studying the role of BRCA1 in meiotic DNA end resection either. In male *Stra8-GFPCre* mice, the GFP-Cre fusion protein is expressed at the same time when STRA8 is expressed in differentiating spermatogonia (30). Male *Brca1*$^{f/-}$ *Stra8-GFPCre* mice are infertile, but unexpectedly, no cells in meiotic prophase could be found in the testes of these mice, making it impossible to study the role of BRCA1 in meiotic DNA end resection using these mice. Therefore, additional mouse models are required to clarify whether BRCA1 has any function in meiotic DNA end resection.

It remains elusive how BRCA1 promotes the loading of meiotic recombinases to DSBs. In somatic cells, BRCA1 directly interacts with PALB2, which binds and loads the BRCA2-RAD51 complex to DSBs (39–41). However, disrupting BRCA1-PALB2 interaction in *Palb2*$^{CC6/CC6}$ mice only mildly compromises meiotic recombination (42). The recruitment of BRCA2-RAD51/DMC1 complex to meiotic DSBs requires meiosis-specific protein MEILB2 and BRME1 (43–46), but the role of PALB2 in this process is unclear. Together with the observation that BRCA1's localization on unsynapsed chromosome axes is not restricted to DSB sites, BRCA1 probably promotes the loading of meiotic recombinases to DSBs through a unique mechanism that warrants further investigation.

BRCA1-Dependent Chromosome Asynapsis Checkpoint Plays a Predominant Role in Eliminating Recombination-Defective Oocytes. Besides promoting meiotic recombination, we identify a function of BRCA1 in eliminating recombination-defective oocytes. Unrepaired DSBs can directly activate the DNA damage checkpoint to trigger the elimination of these oocytes (5). Interestingly, BRCA1 does not regulate the DNA damage checkpoint in oocytes, although it promotes DNA damage checkpoints in somatic cells (21, 47). The different DNA damage responses between somatic cells and oocytes might cause such differences. Equipped with multiple pathways for DNA damage repair, somatic cells can tolerate certain levels of DNA damage without compromising viability. The major DNA damage checkpoints in somatic cells are cell cycle checkpoints, which prevent cell cycle progression until DNA damage is repaired. On the contrary, DNA damage does not activate cell cycle checkpoints in oocytes because oocytes are arrested at dictyate stages of the meiotic prophase and won't resume cell cycle progression until puberty. Instead, oocytes are extremely sensitive to DNA damage. They can be eliminated by a very low dose of IR (5–8), suggesting that the primary purpose of the DNA damage checkpoint in oocytes is to trigger oocyte elimination to preserve genomic integrity. Therefore, despite sharing some core proteins such as CHK2, the regulation of the DNA damage checkpoint in oocytes differs significantly from that in somatic cells.

Despite being dispensable for the DNA damage checkpoint, BRCA1 promotes the activation of chromosome asynapsis checkpoint to eliminate recombination-defective oocytes. *Brca1*$^{-/-}$ efficiently rescues the survival of *Dmc1*$^{-/-}$ oocytes, suggesting that the chromosome asynapsis checkpoint is important for eliminating recombination-defective oocytes. Compared with *Brca1*$^{-/-}$, *Hormad1*$^{-/-}$ rescues the survival of *Dmc1*$^{-/-}$ oocytes even more efficiently (19). Preferentially located at unsynapsed chromosome axes and regulating BRCA1's localization, HORMAD1 is required for the chromosome asynapsis checkpoint, but it also regulates the DNA damage checkpoint (7). Since HORMAD1 is an accessory component of DSB formation machinery (15), *Dmc1*$^{-/-}$ *Hormad1*$^{-/-}$ oocytes have fewer DSBs to start with. DSB repair is also promoted as IS recombination is no longer suppressed in *Dmc1*$^{-/-}$ *Hormad1*$^{-/-}$ oocytes (7, 19). Therefore, HORMAD1 probably functions in both the DNA damage checkpoint and the chromosome asynapsis checkpoint, and its loss compromises both checkpoints and robustly rescues the survival of recombination-defective oocytes. Although functioning downstream of HORMAD1 on unsynapsed chromosome axes, loss of BRCA1 neither compromises DSB formation nor

promotes IS recombination. Together with the observation that BRCA1 is dispensable for DNA damage checkpoint in oocytes, our study suggests that *Brca1*$^{-/-}$ only compromises chromosome asynapsis checkpoint. Therefore, our study indicates that chromosome asynapsis checkpoint can directly trigger the elimination of recombination-defective oocytes independently of the DNA damage checkpoint. We propose that CHK2-dependent DNA damage checkpoint and BRCA1-dependent chromosome asynapsis checkpoint surveil unrepaired DSBs and chromosome asynapsis, respectively, and these two checkpoints function together to eliminate recombination-defective oocytes (Fig. 8). Since *Brca1*$^{-/-}$ rescues the survival of *Dmc1*$^{-/-}$ oocytes far more efficiently than *Chk2*$^{-/-}$, our study strongly suggests that chromosome asynapsis checkpoint, but not DNA damage checkpoint, plays a predominant role in eliminating recombination-defective oocytes (Fig. 8). To clarify the relationship between these two checkpoints, it will be interesting to examine whether BRCA1-dependent chromosome asynapsis checkpoint can eliminate oocytes with recombination defects but intact synapsis, such as *Trip13*^{RRB047} oocytes (48, 49).

Given that *Spo11*$^{-/-}$ oocytes are eliminated in the absence of programmed DSBs, it has been proposed that chromosome asynapsis directly triggers the elimination of these oocytes (4). Unexpectedly, foci of DNA damage repair proteins are found in *Spo11*$^{-/-}$ oocytes (6, 34, 35), and *Chk2*$^{-/-}$ partially rescues the survival of *Spo11*$^{-/-}$ oocytes (6). These observations challenge the role of chromosome asynapsis checkpoint in oocyte elimination and give rise to the idea that DSBs of unknown origins activate CHK2-dependent DNA damage checkpoint to eliminate *Spo11*$^{-/-}$ oocytes. However, thorough analysis in a recent study reveals that the number of DSBs in *Spo11*$^{-/-}$ oocytes is even fewer than in WT oocytes, questioning the contribution of DNA damage checkpoint

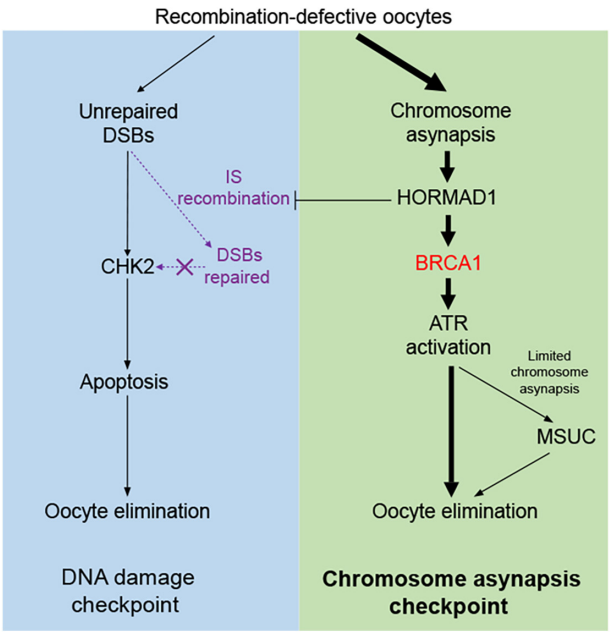

Fig. 8. Working model: chromosome asynapsis checkpoint plays a predominant role in eliminating recombination-defective oocytes. CHK2-dependent DNA damage checkpoint (*Left*) and BRCA1-dependent chromosome asynapsis checkpoint (*Right*) surveil unrepaired DSBs and chromosome asynapsis, respectively, and these two checkpoints function together to eliminate recombination-defective oocytes. After being recruited to unsynapsed chromosome axes by HORMAD1, BRCA1 activates chromosome asynapsis checkpoint by promoting ATR activity. HORMAD1 probably functions in both checkpoints since it also suppresses IS recombination such that DSBs persist and activate the DNA damage checkpoint (purple dotted arrow). The observation that *Brca1*$^{-/-}$ rescues the survival of *Dmc1*$^{-/-}$ oocytes far more efficiently than *Chk2*$^{-/-}$ suggests that chromosome asynapsis checkpoint plays a predominant role in eliminating recombination-defective oocytes.

in eliminating *Spo11*$^{-/-}$ oocytes (9). We show that *Brca1*$^{-/-}$ efficiently rescues the survival of *Spo11*$^{-/-}$ oocytes. Since BRCA1 has no role in IS recombination or DNA damage checkpoint, our study suggests that chromosome asynapsis checkpoint can directly trigger the elimination of asynaptic *Spo11*$^{-/-}$ oocytes independently of DNA damage checkpoint, regardless of DSB levels in these oocytes.

BRCA1-Dependent Chromosome Asynapsis Checkpoint Promotes Oocyte Elimination Independently of MSUC. In spermatocytes, BRCA1 is located at unsynapsed chromosome axes in the XY body and promotes MSCI (27). Similarly, it is believed that BRCA1 activates MUSC and promotes the elimination of oocytes with limited chromosomes asynapsis (13). When chromosome asynapsis increases, the signal of BRCA1 on unsynapsed chromosome axes becomes fainter and nonuniform, accompanied by the decreased intensity of markers of silencing chromatin (13). Based on this observation, it is proposed that limited BRCA1 fails to activate MSUC to eliminate oocytes with pervasive chromosome asynapsis. In our study, the signals of both BRCA1 and ATR substrate p-HORMAD2(S271) are also nonuniform on unsynapsed chromosome axes in *Dmc1*$^{-/-}$ oocytes, but BRCA1 can promote the elimination of *Dmc1*$^{-/-}$ oocytes. Therefore, despite being inadequate for MSUC, the amount of BRCA1 is sufficient for activating the chromosome asynapsis checkpoint in oocytes with pervasive chromosome asynapsis, suggesting that BRCA1-dependent chromosome asynapsis checkpoint promotes the elimination of these oocytes independently of MSUC.

Given the more intense and uniform signals of BRCA1 in oocytes with limited chromosomes asynapsis, BRCA1 should also promote ATR activity on unsynapsed chromosome axes and active the chromosome asynapsis checkpoint as it does in oocytes with pervasive chromosome asynapsis. MSUC and chromosome asynapsis checkpoint are likely two events downstream of BRCA1-dependent ATR activity (Fig. 8). While MSUC is a rapid local event that is activated only by strong BRCA1-dependent ATR activity in oocytes with limited chromosome asynapsis, chromosome asynapsis checkpoint is a slower global event that is activated by even weaker BRCA1-dependent ATR activity in oocytes with all levels of chromosome asynapsis.

A previous study suggests that silencing oogenesis-essential genes is required for MSUC to trigger oocyte elimination (14). If this idea is true, other mechanisms should exist to eliminate oocytes with asynapsis on chromosomes that carry no oogenesis-essential genes. It is possible that rapid MSUC activation specifically eliminates oocytes with limited asynapsis on chromosomes that carry oogenesis-essential genes, and slower chromosome asynapsis checkpoint activation eliminates oocytes with all levels of chromosome asynapsis before the primordial follicle pool is generated. Therefore, the BRCA1-dependent chromosome asynapsis checkpoint could be a more general mechanism in oocyte elimination.

HORMAD1-BRCA1-ATR Pathway in Chromosome Asynapsis Checkpoint. Consistent with its function in chromosome asynapsis checkpoint but not in DNA damage checkpoint, BRCA1's localization on unsynapsed chromosome axes in oocytes is not restricted to DSB sites and is independent of DSB formation. Although BRCA1's signal is nonuniform on unsynapsed chromosome axes in *Dmc1*$^{-/-}$ oocytes, it is distinct from the RPA2 foci representing DSB sites that scatter along chromosome axes. In spermatocytes, the localization of BRCA1 at the unsynapsed chromosome axes in the XY body does not require proteins essential for its recruitment to DSB sites in somatic cells (50). HORMAD1, a key protein in chromosome asynapsis

surveillance, is required for BRCA1's localization at the unsynapsed chromosome axes in oocytes but not vice versa. Collectively, studies in both spermatocytes and oocytes suggest that BRCA1 has a unique function in chromosome asynapsis surveillance in the meiotic prophase, which is distinct from its canonical functions at the DSB site in somatic cells. Future studies are required to reveal the molecular mechanism that underlies the recruitment of BRCA1 to unsynapsed chromosome axes by HORMAD1.

HORMAD2 is another protein that preferentially localizes at unsynapsed chromosome axes in a HORMAD1-dependent manner (16). Like BRCA1, HORMAD2 is required for MSCI in spermatocytes, but there are opposing views on whether HORMAD2 regulates BRCA1's localization in the XY body (16, 17). Unlike BRCA1, HORMAD2 is dispensable for meiotic recombination or female fertility (16, 17). Although HORMAD2 has been implicated to function in chromosome asynapsis checkpoint, *Hormad2*$^{-/-}$ poorly rescues the survival of *Dmc1*$^{-/-}$ oocytes (6, 16), suggesting that HORMAD2 is not as crucial as BRCA1 in eliminating recombination-defective oocytes. The functional relationship between HORMAD2 and BRCA1 in chromosome asynapsis checkpoint in oocytes requires further investigation.

Although BRCA1 and ATR are localized at unsynapsed chromosome axes in oocytes, their functions and relationship in eliminating asynaptic oocytes have never been demonstrated. Our study reveals the role of BRCA1 in promoting ATR activity at unsynapsed chromosome axes in oocytes, suggesting that BRCA1-dependent ATR activity is likely essential for chromosome asynapsis checkpoint activation and oocyte elimination. To consolidate this idea, it will be necessary to examine whether *Atr*$^{-/-}$ robustly rescues the survival of *Dmc1*$^{-/-}$ oocytes in the future. Since ATR might have multiple substrates on unsynapsed chromosome axes, it will also be challenging to identify the critical substrates that mediate ATR's function in chromosome asynapsis checkpoint in oocytes. For example, p-HORMAD2(S271) should not be the critical substrate, as *Hormad2*$^{-/-}$ poorly rescues the survival of *Dmc1*$^{-/-}$ oocytes (6, 16). Nevertheless, elucidating the function of ATR on unsynapsed chromosome axes will help to gain insight into the chromosome asynapsis checkpoint in oocytes.

Materials and Methods

Mice. *Brca1*$^{f/f}$ mice (Strain No. 01XB8) were obtained from NCI Mouse Repository. *Brca1*$^{+/-}$ mice were generated by crossing *Brca1*$^{f/f}$ mice with *Ddx4-Cre* mice (Strain No. 006954) that were obtained from The Jackson Laboratory. *53bp1*$^{-/-}$ mice (Strain No. 006495) were obtained from The Jackson Laboratory. *Brca1*$^{-/-}$ *53bp1*$^{-/-}$ mice were generated as described previously (28). *Hormad1*$^{-/-}$ mice were obtained from RIKEN BRC (Strain No. CDB0575K). *Chk2*$^{-/-}$mice were obtained from GemPharmatech (Strain No. T027449). *Dmc1*$^{-/-}$ mice were kind gifts of Hongbin Liu (Shandong University). *Stra8-GFPCre* mice were kind gifts of Ming-Han Tong (Chinese Academy of Sciences) (30). *Spo11*$^{-/-}$ mice were kind gifts of Qinghua Shi (University of Science and Technology of China) (51). All animals were maintained under an appropriately controlled environment (light and temperature) with easy access to food and water. All experimental procedures were approved by Zhejiang University Animal Care and Use Committee (File No. ZJU20190144 and ZJU20220228).

Fertility Test. *Brca1*$^{-/-}$ *53bp1*$^{-/-}$ male and female mice, *Brca1*$^{f/-}$ *Stra8-GFPCre* female mice and their corresponding control mice were mated with WT adult male or female mice once they reached 8 wk old. Litter sizes were determined by counting pups at birth for 3 consecutive months.

Histological Analysis. Ovaries were fixed overnight in 4% PFA at 4 °C. Testes and epididymides were fixed in Bouin's solution for 24 h at room temperature. The fixed tissues were dehydrated through a series of increasing concentrations of ethanol and then embedded in paraffin for serial sectioning at 5 μm thickness. The sections were stained with hematoxylin and eosin (H&E). For follicle number quantification of PD21 and PD60 female ovary, follicle numbers were counted in every fifth section. For follicle number quantification of PD4 female ovary, follicle numbers were quantified by counting the MVH-positive cell number in the central section of the ovary. Only one ovary per animal was used for follicle quantification. Histological images were obtained from slides digitized by the Grundium Ocus® microscope slide scanners (OCUS01, Grundium).

Analysis of Fertilization and Early Embryonic Development. PD21 female mice were injected intraperitoneally with 5 IU of PMSG (Ningbo Sansheng Biological Technology) and 5 IU of hCG (Ningbo Sansheng Biological Technology) 44 h apart. Immediately after the injection of hCG, female mice were placed individually with WT adult male mice. Successful mating was confirmed by the presence of vaginal plugs. For fertilization analysis, zygotes were collected 24 h after hCG injection. Successful fertilization was determined by the presence of two pronuclei. For early embryonic development analysis, zygotes and embryos were collected at 0.5, 1.5, 2.5, and 3.5 d after fertilization. The unfertilized oocytes after the zygote stage were excluded during analysis.

Preparation of Oocyte Chromosome Spreads. Oocytes were exposed to acidic M2 medium for 10 min at 37 °C to remove zona pellucida. Zonal pellucida-free oocytes were dropped onto a clean glass slide, fixed with spreading buffer [1% paraformaldehyde (PFA), 0.15% Triton X-100, and 3 mM DTT] for 30 min, and air dried.

Preparation of Meiotic Spreads. For spreads of oocytes at the meiotic prophase, ovaries were dissected from fetal or newborn female mice. Ovaries were incubated in hypotonic extraction buffer (30 mM Tris-HCl pH 8.0, 50 mM sucrose, and 17 mM sodium citrate) for 30 min and were then transferred into droplets of 100 mM sucrose buffer. Oocytes were released by puncturing the ovaries with needles and were incubated in 100 mM sucrose buffer for 10 min. After removing big pieces of tissue, the cell suspension was mixed with an equal volume of fixative buffer (1% PFA, 0.15% Triton X-100, and 10 mM borate buffer, pH 9.2), smeared onto coverslips, and air dried.

For spreads of spermatocytes at the meiotic prophase, testes were dissected from PD28 males. After removing tunica albuginea, testes were digested in collagenase IV solution (1 mg/mL) for 20 min. Cell pellets were resuspended in hypotonic extraction buffer for 10 min and then in 100 mM sucrose buffer for 5 min. The cell suspension was then mixed with an equal volume of fixative buffer, smeared onto coverslips, and air-dried.

Immunofluorescent (IF) Staining and Imaging. For IF staining of chromosome spreads and meiotic spreads, coverslips were blocked with 5% BSA for 30 min at room temperature and subsequently incubated with primary antibodies. Coverslips were washed in phosphate-buffered saline (PBS) three times and were then incubated with Alexa Fluor–labeled secondary antibodies. After washing in PBS three times, coverslips were stained with Hoechst 33342 and mounted with antifade reagent. Images were taken using a fluorescence microscope with a 60× immersion oil lens and CCD camera (ECLIPSE Ti2-E, Nikon).

For IF staining of oocytes, germinal-vesicle stage oocytes from PD21 female mice were harvested in M2 medium 44 h after PMSG injection and cultured in minidrops of M16 medium covered with mineral oil for additional 8 h at 37 °C in a 5% CO_2 atmosphere. IF staining of oocytes at the MI stage was similarly performed as described above. Images were taken using a laser scanning confocal microscope (STELLARIS 5, Leica Microsystems).

For IF staining of paraffin sections of ovaries, sections were deparaffinized, rehydrated, and incubated with antigen retrieval buffer (10 mM Sodium Citrate with 0.05% Tween, pH 6.0) at 95 °C for 30 min. For IF staining in frozen sections of ovaries or gonads, ovaries or gonads were fixed overnight in 4% PFA solution at 4 °C, dehydrated in 30% sucrose solution, embedded in OCT, and stored in −80 °C before sectioning at 10 μm thickness. IF staining of ovarian sections was similarly performed as described above. Images were taken using a laser scanning confocal microscope (STELLARIS 5, Leica Microsystems). Antibody information is listed in *SI Appendix*, Table S1.

Ionizing Radiation (IR). To investigate the IR sensitivity of oocytes, PD3 female mice were exposed to a single dose of 0.45 Gy IR, and their ovaries were isolated for histological analysis 1 wk after IR. To investigate the DNA damage signaling pathways in

oocytes, PD3 female mice were exposed to a single dose of 3 Gy IR, and their ovaries were isolated for histological analysis 1 h after IR or for western blotting 2 h after IR.

Western Blotting. Ovaries were collected and stored at −80 °C. Ovaries were homogenized and lysed in RIPA buffer with a protease inhibitor cocktail (P8340, Sigma) using an ultrasonic cell disruptor (SCIENTZ08-II, Ningbo Scientz Biotechnology Company). Proteins were separated by SDS–PAGE and transferred onto PVDF membranes. The membranes were blocked by 5% nonfat milk in PBST (PBS containing 20% Triton X-100), incubated overnight with primary antibodies at 4 °C, washed with PBST, and incubated with horseradish peroxidase–linked secondary antibodies. After washing with PBST, the membranes were analyzed using an enhanced chemiluminescence system. Antibody information is listed in *SI Appendix*, Table S1.

Statistical Analysis. Statistical analysis was performed by GraphPad Prism 6, and the results were presented as means ± SD. At least three independent samples were included in each experiment. To calculate statistical significance between different groups, two-tailed unpaired Student's *t* tests were performed.

Data, Materials, and Software Availability. All study data are included in the article and/or *SI Appendix*.

ACKNOWLEDGMENTS. We thank Hongbin Liu, Qinghua Shi, and Ming-Han Tong for sharing mouse strains and Attila Tóth for sharing antibodies. We thank Quanfeng Zhu and Shenghui Hong for helping with mouse strain rederivation. We thank Chao Bi and Xiaoli Hong from the Core Facilities, Zhejiang University School of Medicine for their technical support. This work is funded by the Key Research and Development Program of Zhejiang Province (2021C03100), Zhejiang Provincial Natural Science Foundation (LQ21C120001 and LZ21H040001), and National Natural Science Foundation of China (32070829, 32100676, and 32370900).

Author affiliations: [a]Key Laboratory of Reproductive Genetics (Ministry of Education) and Women's Reproductive Health Laboratory of Zhejiang Province, Women's Hospital, Zhejiang University School of Medicine, Hangzhou 310006, China; [b]Institute of Translational Medicine, Zhejiang University School of Medicine, Hangzhou 310029, China; [c]Zhejiang Provincial Key Laboratory of Precision Diagnosis and Therapy for Major Gynecological Diseases, Women's Hospital, Zhejiang University School of Medicine, Hangzhou 310006, China; [d]Department of Reproductive Endocrinology, Women's Hospital, Zhejiang University School of Medicine, Hangzhou 310006, China; and [e]Zhejiang University Cancer Center, Hangzhou 310029, China

Author contributions: Y.L., Y.Z., and L.-Y.L. designed research; L.B., P.L., Y.X., X.J., J.C., L.S., and Z.L. performed research; L.B., P.L., Y.L., Y.Z., and L.-Y.L. analyzed data; and L.B., P.L., and L.-Y.L. wrote the paper.

1. N. Hunter, Meiotic recombination: The essence of heredity. *Cold Spring Harb. Perspect. Biol.* **7**, a016618 (2015).
2. F. Baudat, Y. Imai, B. de Massy, Meiotic recombination in mammals: Localization and regulation. *Nat. Rev. Genet.* **14**, 794–806 (2013).
3. D. Zickler, N. Kleckner, Recombination, pairing, and synapsis of homologs during meiosis. *Cold Spring Harb. Perspect. Biol.* **7**, a016626 (2015).
4. M. Di Giacomo *et al.*, Distinct DNA-damage-dependent and -independent responses drive the loss of oocytes in recombination-defective mouse mutants. *Proc. Natl. Acad. Sci. U.S.A.* **102**, 737–742 (2005).
5. E. Bolcun-Filas, V. D. Rinaldi, M. E. White, J. C. Schimenti, Reversal of female infertility by Chk2 ablation reveals the oocyte DNA damage checkpoint pathway. *Science* **343**, 533–536 (2014).
6. V. D. Rinaldi, E. Bolcun-Filas, H. Kogo, H. Kurahashi, J. C. Schimenti, The DNA damage checkpoint eliminates mouse oocytes with chromosome synapsis failure. *Mol. Cell* **67**, 1026–1036.e1022 (2017).
7. H. Qiao *et al.*, Impeding DNA break repair enables oocyte quality control. *Mol. Cell* **72**, 211–221. e213 (2018).
8. E. ElInati *et al.*, The BCL-2 pathway preserves mammalian genome integrity by eliminating recombination-defective oocytes. *Nat. Commun.* **11**, 2598 (2020).
9. R. Ravindranathan, K. Raveendran, F. Papanikos, P. A. San-Segundo, A. Toth, Chromosomal synapsis defects can trigger oocyte apoptosis without elevating numbers of persistent DNA breaks above wild-type levels. *Nucleic Acids Res.* **50**, 5617–5634 (2022).
10. V. D. Rinaldi, J. C. Bloom, J. C. Schimenti, Oocyte elimination through DNA damage signaling from CHK1/CHK2 to p53 and p63. *Genetics* **215**, 373–378 (2020).
11. J. B. Kerr *et al.*, DNA damage-induced primordial follicle oocyte apoptosis and loss of fertility require TAp63-mediated induction of Puma and Noxa. *Mol. Cell* **48**, 343–352 (2012).
12. A. Martinez-Marchal *et al.*, The DNA damage response is required for oocyte cyst breakdown and follicle formation in mice. *PLoS Genet.* **16**, e1009067 (2020).
13. A. Kouznetsova *et al.*, BRCA1-mediated chromatin silencing is limited to oocytes with a small number of asynapsed chromosomes. *J. Cell Sci.* **122**, 2446–2452 (2009).
14. J. M. Cloutier *et al.*, Histone H2AFX links meiotic chromosome asynapsis to prophase I oocyte loss in mammals. *PLoS Genet.* **11**, e1005462 (2015).
15. K. Daniel *et al.*, Meiotic homologue alignment and its quality surveillance are controlled by mouse HORMAD1. *Nat. Cell Biol.* **13**, 599–610 (2011).
16. L. Wojtasz *et al.*, Meiotic DNA double-strand breaks and chromosome asynapsis in mice are monitored by distinct HORMAD2-independent and -dependent mechanisms. *Genes Dev.* **26**, 958–973 (2012).
17. H. Kogo *et al.*, HORMAD2 is essential for synapsis surveillance during meiotic prophase via the recruitment of ATR activity. *Genes Cells* **17**, 897–912 (2012).
18. H. Kogo *et al.*, HORMAD1-dependent checkpoint/surveillance mechanism eliminates asynaptic oocytes. *Genes Cells* **17**, 439–454 (2012).
19. Y. H. Shin, M. M. McGuire, A. Rajkovic, Mouse HORMAD1 is a meiosis i checkpoint protein that modulates DNA double- strand break repair during female meiosis. *Biol. Reprod.* **89**, 29 (2013).
20. S. C. Kowalczykowski, An overview of the molecular mechanisms of recombinational DNA repair. *Cold Spring Harb. Perspect. Biol.* **7** (2015).
21. M. S. Huen, S. M. Sy, J. Chen, BRCA1 and its toolbox for the maintenance of genome integrity. *Nat. Rev. Mol. Cell Biol.* **11**, 138–148 (2010).
22. W. Zhao, C. Wiese, Y. Kwon, R. Hromas, P. Sung, The BRCA tumor suppressor network in chromosome damage repair by homologous recombination. *Annu. Rev. Biochem.* **88**, 221–245 (2019).
23. M. Tarsounas, P. Sung, The antitumorigenic roles of BRCA1-BARD1 in DNA repair and replication. *Nat. Rev. Mol. Cell Biol.* **21**, 284–299 (2020).
24. Y. Liu, L. Y. Lu, BRCA1: A key player at multiple stages of homologous recombination in DNA double-strand break repair. *Genome Instab. Dis.* **2**, 164–174 (2021).
25. X. Xu, O. Aprelikova, P. Moens, C. X. Deng, P. A. Furth, Impaired meiotic DNA-damage repair and lack of crossing-over during spermatogenesis in BRCA1 full-length isoform deficient mice. *Development* **130**, 2001–2012 (2003).
26. T. J. Broering *et al.*, BRCA1 establishes DNA damage signaling and pericentric heterochromatin of the X chromosome in male meiosis. *J. Cell Biol.* **205**, 663–675 (2014).
27. J. M. Turner *et al.*, BRCA1, histone H2AX phosphorylation, and male meiotic sex chromosome inactivation. *Curr. Biol.* **14**, 2135–2142 (2004).
28. J. Chen *et al.*, 53BP1 loss rescues embryonic lethality but not genomic instability of BRCA1 total knockout mice. *Cell Death Differ.* **27**, 2552–2567 (2020).
29. L. J. Huber *et al.*, Impaired DNA damage response in cells expressing an exon 11-deleted murine Brca1 variant that localizes to nuclear foci. *Mol. Cell Biol.* **21**, 4005–4015 (2001).
30. Z. Lin *et al.*, Mettl3-/Mettl14-mediated mRNA N(6)-methyladenosine modulates murine spermatogenesis. *Cell Res.* **27**, 1216–1230 (2017).
31. H. Royo *et al.*, ATR acts stage specifically to regulate multiple aspects of mammalian meiotic silencing. *Genes Dev.* **27**, 1484–1494 (2013).
32. T. Fukuda *et al.*, Phosphorylation of chromosome core components may serve as axis marks for the status of chromosomal events during mammalian meiosis. *PLoS Genet.* **8**, e1002485 (2012).
33. S. K. Mahadevaiah *et al.*, Extensive meiotic asynapsis in mice antagonises meiotic silencing of unsynapsed chromatin and consequently disrupts meiotic sex chromosome inactivation. *J. Cell Biol.* **182**, 263–276 (2008).
34. S. Malki, G. W. van der Heijden, K. A. O'Donnell, S. L. Martin, A. Bortvin, A role for retrotransposon LINE-1 in fetal oocyte attrition in mice. *Dev. Cell* **29**, 521–533 (2014).
35. F. Carofiglio *et al.*, SPO11-independent DNA repair foci and their role in meiotic silencing. *PLoS Genet.* **9**, e1003538 (2013).
36. S. F. Bunting *et al.*, 53BP1 inhibits homologous recombination in Brca1-deficient cells by blocking resection of DNA breaks. *Cell* **141**, 243–254 (2010).
37. Y. Liu, L. Y. Lu, BRCA1 and homologous recombination: Implications from mouse embryonic development. *Cell Biosci.* **10**, 49 (2020).
38. J. Paiano *et al.*, ATM and PRDM9 regulate SPO11-bound recombination intermediates during meiosis. *Nat. Commun.* **11**, 857 (2020).
39. S. M. Sy, M. S. Huen, J. Chen, PALB2 is an integral component of the BRCA complex required for homologous recombination repair. *Proc. Natl. Acad. Sci. U.S.A.* **106**, 7155–7160 (2009).
40. F. Zhang *et al.*, PALB2 links BRCA1 and BRCA2 in the DNA-damage response. *Curr. Biol.* **19**, 524–529 (2009).
41. B. Xia *et al.*, Control of BRCA2 cellular and clinical functions by a nuclear partner, PALB2. *Mol. Cell* **22**, 719–729 (2006).
42. S. Simhadri *et al.*, Male fertility defect associated with disrupted BRCA1-PALB2 interaction in mice. *J. Biol. Chem.* **289**, 24617–24629 (2014).
43. J. Zhang, Y. Fujiwara, S. Yamamoto, H. Shibuya, A meiosis-specific BRCA2 binding protein recruits recombinases to DNA double-strand breaks to ensure homologous recombination. *Nat. Commun.* **10**, 722 (2019).
44. I. Brandsma *et al.*, HSF2BP interacts with a conserved domain of BRCA2 and is required for mouse spermatogenesis. *Cell Rep.* **27**, 3790–3798.e3797 (2019).
45. J. Zhang *et al.*, The BRCA2-MEILB2-BRME1 complex governs meiotic recombination and impairs the mitotic BRCA2-RAD51 function in cancer cells. *Nat. Commun.* **11**, 2055 (2020).
46. K. Takemoto *et al.*, Meiosis-specific C19orf57/4930432K21Rik/BRME1 modulates localization of RAD51 and DMC1 to DSBs in mouse meiotic recombination. *Cell Rep.* **31**, 107686 (2020).
47. C. X. Deng, BRCA1: Cell cycle checkpoint, genetic instability, DNA damage response and cancer evolution. *Nucleic Acids Res.* **34**, 1416–1426 (2006).
48. X. C. Li, J. C. Schimenti, Mouse pachytene checkpoint 2 (trip13) is required for completing meiotic recombination but not synapsis. *PLoS Genet.* **3**, e130 (2007).
49. I. Roig *et al.*, Mouse TRIP13/PCH2 is required for recombination and normal higher-order chromosome structure during meiosis. *PLoS Genet.* **6**, e1001062 (2010).
50. L. Y. Lu, Y. Xiong, H. Kuang, G. Korakavi, X. Yu, Regulation of the DNA damage response on male meiotic sex chromosomes. *Nat. Commun.* **4**, 2105 (2013).
51. P. J. Romanienko, R. D. Camerini-Otero, The mouse Spo11 gene is required for meiotic chromosome synapsis. *Mol. Cell* **6**, 975–987 (2000).